DISCLAIMER

This report was prepared as an account of work sponsored by an agency of the United States Government. Neither the United States Government nor any agency thereof, nor any of their employees, makes any warranty, express or implied, or assumes any legal liability or responsibility for the accuracy, completeness, or usefulness of any information, apparatus, product, or process disclosed, or represents that its use would not infringe privately owned rights. Reference herein to any specific commercial product, process, or service by trade name, trademark, manufacturer, or otherwise does not necessarily constitute or imply its endorsement, recommendation, or favoring by the United States Government or any agency thereof. The views and opinions of authors expressed herein do not necessarily state or reflect those of the United States Government or any agency thereof. Reference herein to any social initiative (including but not limited to Diversity, Equity, and Inclusion (DEI); Community Benefits Plans (CBP); Justice 40; etc.) is made by the Author independent of any current requirement by the United States Government and does not constitute or imply endorsement, recommendation, or support by the United States Government or any agency thereof.

SANDIA REPORT
SAND2024-16813
Printed December 2024

Sandia National Laboratories

Notes on Synthetic Aperture Radar Image Quality

Armin W. Doerry and Douglas L. Bickel

Prepared by
Sandia National Laboratories
Albuquerque, New Mexico
87185 and Livermore,
California 94550

Issued by Sandia National Laboratories, operated for the United States Department of Energy by National Technology & Engineering Solutions of Sandia, LLC.

Available to DOE and DOE contractors from
U.S. Department of Energy
Office of Scientific and Technical Information
P.O. Box 62
Oak Ridge, TN 37831

Telephone: (865) 576-8401
Facsimile: (865) 576-5728
E-Mail: reports@osti.gov
Online ordering: http://www.osti.gov/scitech

Available to the public from
U.S. Department of Commerce
National Technical Information Service
5301 Shawnee Rd
Alexandria, VA 22312

Telephone: (800) 553-6847
Facsimile: (703) 605-6900
E-Mail: orders@ntis.gov
Online order: https://classic.ntis.gov/help/order-methods/

Notes on Synthetic Aperture Radar Image Quality

Armin W. Doerry, Douglas L. Bickel

Abstract

Synthetic Aperture Radar (SAR) creates an image of a target scene by coherently processing radar echo returns collected along a flightpath. The quality of the SAR image is inextricably linked to the utility of the image for exploitation supporting the task at hand. Aspects of quality include the fidelity with which it can render the scene being imaged, to include the system's Impulse Response (IPR) and underlying noise levels/characteristics. Other factors also impact utility, and hence quality, such as imaging geometry and metadata. In addition, subjective measures of SAR image quality are also employed, such as NIIRS, especially by the radar tasking and exploitation communities.

Acknowledgements

The authors wish to thank Aimee Shore for her detailed review and helpful suggestions for this report.

This report is the result of an unfunded Research and Development investigation.

Sandia National Laboratories is a multimission laboratory managed and operated by National Technology & Engineering Solutions of Sandia LLC, a wholly owned subsidiary of Honeywell International Inc. for the U.S. Department of Energy's National Nuclear Security Administration under contract DE-NA0003525.

Contents

List of Figures

List of Tables

Acronyms and Definitions

1-D, 2-D, 3-D	1- 2- 3- Dimensional
ADC	Analog-to-Digital Converter
AESA	Active Electronically Steered Array
AGC	Automatic Gain Control
AM	Amplitude Modulation
AMBR	Ambiguity Ratio
ATD	Automated Target Detection
ATR	Automatic Target Recognition
AWGN	Additive White Gaussian Noise
DAC	Digital-to-Analog Converter
GIQE	General Image-Quality Equation
IPR	Impulse Response
I/Q	In-phase and Quadrature phase
ITU	International Telecommunications Union
IDF	Image Domain Filtering
ISLR	Integrated Sidelobe Ratio
KPP	Key Performance Parameter(s)
LFM	Linear Frequency Modulated [chirp]
LO	Local Oscillator
MII	Multiple Image Integration
MNR	Multiplicative Noise Ratio
MTI	Moving Target Indicator
NGA	National Geospatial-Intelligence Agency
NIIRS	National Image Interpretability Rating Scale
PFA	Polar Format Algorithm
PLL	Phase-Locked Loop
POSM	Plain Old SAR Mode
PM	Phase Modulation
PRF	Pulse Repetition Frequency
PSD	Power Spectral Density
PSF	Point Spread Function
PSLR	Peak Sidelobe Ratio
PSR	Point Scatterer Response
QNR	Quantization Noise Ratio
RCS	Radar Cross Section
RNIIRS	Radar-NIIRS
RX	Receive, Receiver
SAR	Synthetic Aperture Radar
SNR	Signal-to-Noise Ratio
SRP	Scene Reference Point
STALO	Stable Local Oscillator
TTD	True-Time-Delay
TX	Transmit, Transmitter

Foreword

This report details the results of an academic study. It does not intend to exemplify any modes, methodologies, or techniques employed by any specific system, operational or experimental. Any resemblance to such is accidental and inadvertent.

Classification

The specific mathematics and algorithms presented herein do not bear any release restrictions or distribution limitations.

This report formalizes preexisting informal notes and other documentation on the subject matter herein.

This report has been approved as Unclassified – Unlimited Release.

Author Contact Information

Armin Doerry awdoerr@sandia.gov 505-845-8165 www.doerry.us

1 Introduction and Background

Synthetic Aperture Radar (SAR) is a radar modality that creates a spatial map which we typically render as an image, usually of a surface, where pixels in that image represent a function of radar backscatter or reflectivity. SAR images are formed by coherently processing a plurality of radar echoes from a diverse set of perspectives, usually collected along some radar platform's path of motion. It can be cast, and often is cast, as a tomographic technique. As with virtually all conventional imaging techniques, it projects the 3-Dimensional (3-D) scene into a 2-Dimensional (2-D) view. The resulting image created from SAR processing finds utility in all manner of applications, from military, scientific, mapping, resource management, commercial, and academic. An example SAR image is given in Figure 1.

Figure 1. Example Ku-band SAR image of a Sandia National Laboratories test facility in Albuquerque, New Mexico, USA. Relevant parameters are 0.1016 m slant-range and cross-range resolution, nominal 6.858 km slant range, 30.3545 deg grazing angle, and –30 dBsm/m^2 noise floor.

Portfolios of other SAR images can be found in several other publications.[1,2,3,4,5,6]

With the typical SAR output product being an image, the natural question then becomes "How good is it?" That is, "How might we judge the quality of a SAR image?" This question is somewhat difficult to precisely answer, and even more difficult to adequately and fully quantify. We are often left with the vague sentiment "I'll know it when I see it."

Nevertheless, we may from basic principles make some basic observations about quality. For example, we deem it desirable to have a SAR image with high quality, and less desirable to have a SAR image without high quality, i.e., with low quality. Consequently, quality describes whether a SAR image offers to us characteristics which we desire and deem adequate for our purposes. This leads us to the observation that the characteristic of quality is application dependent. We quote Austrian American management consultant Peter Drucker who states "Quality in a service or product is not what you put into it. It is what the customer gets out of it."

An extension of application dependence is the idea of "observer dependence." Specifically, we must acknowledge that direct human exploitation of a SAR image might require different measures of 'goodness' than if we employed machine exploitation of a SAR image.

So, for a SAR image, quality is then some indication of "how well can we see/measure what we want to see/measure?" From this, we may then drill down to some secondary concepts.

Given that a SAR image is a spatial map, we generally desire that it satisfies our notions of what a spatial map ought to be. That is, we expect the image to localize features that ought to be localized, and represent spatial relationships consistent with our intuition. Furthermore, pixel values need to explicably represent a physical characteristic of an associated localized and resolved area within the target scene and to within some calculable error bounds.

Moreover, quality is generally increased with a higher fidelity rendering of the target scene, and also generally increased with a lesser degree of obscuration by ubiquitous noise.

To be sure, SAR image quality has been frequently treated in the literature. We offer several examples but readily acknowledging that this selection is woefully incomplete, and merely representative.

> Clinard presents a survey of image quality measurement techniques for airborne SAR.[7]
>
> Clinard, et al., discuss a number of radar system characteristics affecting SAR image quality.[8]
>
> Mitchel and Marder offer SAR image quality measures which relate to application information requirements and measurement techniques.[9,10]
>
> Martinez and Marchand present a methodology for the analysis of point targets and extended targets in SAR images.[11]
>
> Lu and Sun propose an objective image quality evaluation system with a set of parameters and relevant measurements that are mainly based on SAR image itself.[12]

Vespe and Greidanus discuss relevant quality issues of satellite SAR images related to maritime applications.[13]

Mitchel, et al., discuss an image quality model based on a number of image parameters.[14]

In this report we will discuss SAR image characteristics that will impact a perception of quality. Although as previously discussed, image quality is ultimately an attribute judged by a user, as radar design engineers we nevertheless need to anticipate factors that will impact the user's judgement of quality. Herein we will necessarily discuss image quality from an engineering viewpoint, replete with all the endearing stereotypes associated with being an engineer. (This is where our wives would roll their eyes.)

We will generally limit our discussion to Plain Old SAR Mode (POSM), foregoing any enhanced modes such as those involving polarimetry, interferometry, multistatic operation, or similar complications.

While we may discuss numerical thresholds for some of these SAR image characteristics, we remain mindful that specific thresholds will often be application dependent.

The following sections are arranged as follows.

Section 2 will discuss Signal Fidelity.

Section 3 will discuss Additive Noise.

Section 4 will discuss other factors that impact a perception of quality.

Section 5 will discuss Subjective Measures of Quality.

Section 6 will present some final comments and conclusions.

This report will specifically address SAR images, although many of these observations will apply to other radar modes as well.

"Quality is never an accident. It is always the result of intelligent effort."
– John Ruskin

2 Signal Fidelity

While the term "fidelity" embodies a notion of "faithfulness," or "exactness," we will interpret it here as an indication of how localized a radar echo will render a very local radar target. For our analysis, our local target will be the mythical "point target." The myth is believing that an infinitesimally small isotropic point scatterer will nevertheless exhibit sufficient scattering response to serve as a useful radar target. While such targets are fiction, their theoretical response can be approached with some canonical test reflector shapes, and are useful for radar analysis.[15]

Nevertheless, the point target is mathematically described by a spatial impulse. The radar's response to, and rendering of this target is its Impulse Response (IPR), also called its Point Scatterer Response (PSR). In a 2-D SAR image, the IPR is in fact a 2-D function.† However, frequently only the principal axis cuts of the full 2-D IPR are presented, these being typically referred to for SAR as the range IPR and the orthogonal cross-range (azimuth) IPR.

Recall that a "distortionless system" is one that imparts only constant delay and scaling of a signal, i.e., no distortions as might be due to filtering or altering the spectral content of the signal. Ideally, then an impulse target would generate a faithful impulsive rendering of that target in the SAR image. The extent to which the rendering is itself not precisely and accurately an impulse is due to a performance limitation of the radar and its processing. Therefore, the IPR is a useful measure of the non-ideal nature of the radar itself. This is why we use it.

As prelude to the following discussion, we define the following 2-D impulse function as target truth. We define

$$\delta\left(x-s_x, y-s_y\right) \text{ = 2-D impulse function,} \tag{1}$$

where

$$s_x, s_y \text{ = spatial offset (typically horizontal) of impulse target from spatial origin,} \tag{2}$$

and

$$\delta\left(x-s_x, y-s_y\right)=0 \text{ for } x \neq s_x \text{ or } y \neq s_y, \text{ and}$$

$$\int_{-\infty}^{\infty}\int_{-\infty}^{\infty} \delta\left(x-s_x, y-s_y\right) dxdy = 1. \tag{3}$$

In addition, we identify the 2-D Fourier Transform of an arbitrary 2-D spatial function as

$$H\left(k_x, k_y\right) = \int_{-\infty}^{\infty}\int_{-\infty}^{\infty} h(x,y) e^{-j(k_x x + k_y y)} dxdy, \tag{4}$$

† We offer some comments on 3-D scenes and 3-D wavenumber domains later.

where

$h(x,y)$ = arbitrary spatial function, and

k_x, k_y = angular wavenumbers (spatial frequencies). (5)

We will adopt the convention in this report of using the term "wavenumber" to mean the "angular wavenumber" with units of rad/m, as opposed to the "linear wavenumber" with units of cycles/m. The association of simply "wavenumber" to the angular wavenumber seems to be more common in radar literature,[16] although there are notable exceptions.

Likewise, the corresponding 2-D Inverse Fourier Transform is calculated as

$$h(x,y) = \frac{1}{(2\pi)^2} \int_{-\infty}^{\infty} \int_{-\infty}^{\infty} H(k_x, k_y) e^{+j(k_x x + k_y y)} dk_x dk_y \ . \tag{6}$$

We can use the following shorthand to indicate a Fourier Transform pair.

$$H(k_x, k_y) \Leftrightarrow h(x,y) . \tag{7}$$

We identify $H(k_x, k_y)$ as the wavenumber function. It is analogous to the transfer function in signal processing. The coordinate frame with wavenumber coordinates is often referred to as the "wavenumber domain," or sometimes simply "k-space." We stipulate that k-space is natural to SAR data, since raw SAR data is essentially collected directly in k-space, or at least easily and naturally processed into intermediate data fully represented in k-space.

Accordingly, we identify the Fourier Transform pair for the ideal 2-D impulse function of Eq. (1) as

$$e^{-j(k_x s_x + k_y s_y)} \quad \Leftrightarrow \quad \delta(x - s_x, y - s_y) . \tag{8}$$

We make the important observation that for a true unit impulse target, the spatial frequency content will exhibit a unit modulus for all wavenumbers, and that really means <u>*all*</u> wavenumbers, out to infinity in all directions. Furthermore, any truncation or filtering of the wavenumber function will necessarily alter any ability to render the target as a true impulse. Furthermore yet, any perturbation of the phase linearity of the wavenumber function (with respect to the wavenumbers themselves) will also impact the ability to properly, or optimally render the impulse target.

Basically, the IPR for a radar system is also a measure of the goodness of the wavenumber function. This includes the phase linearity of the radar system over the bands of relevant wavenumbers and any corresponding temporal frequencies.

In the next sections we will parse our analysis of SAR IPR degradation into two main categories,

1. Bounds on the extent of observable wavenumber domain region of support, and
2. Anomalies of the IPR due to perturbation of the wavenumber function within the region of support.

2.1 Wavenumber Region of Support

We first assess the impact of bounding the wavenumber function to a finite enclosed area in the wavenumber domain. Equivalently, we set values for the wavenumber function outside this area to zero. We will initially assume that the wavenumber function within this enclosed area is identical to that of an unperturbed impulse target, but only within this area. We are essentially limiting the spatial (wavenumber) bandwidth of the radar echo. The wavenumber domain region where the effective wavenumber function is allowed to be non-zero is sometimes called the wavenumber "region of support" or "k-space aperture" among other monikers.

For our subsequent analysis, we now define wavenumber region of support as

$$A\left(k_x, k_y\right) = \begin{cases} 1 & \text{within region of support} \\ 0 & \text{else} \end{cases} \tag{9}$$

and calculate the rendering of our 2-D IPR as

$$W_2\left(x - s_x, y - s_y\right) = \frac{1}{\left(2\pi\right)^2} \int_{-\infty}^{\infty} \int_{-\infty}^{\infty} A\left(k_x, k_y\right) e^{-j(k_x s_x + k_y s_y)} e^{+j(k_x x + k_y y)} dk_x dk_y \,. \tag{10}$$

The region of support $A\left(k_x, k_y\right)$ is allowed here to be an arbitrary enclosed area. Its boundaries may be either due to radar collection attributes and/or limitations, or thereafter by cropping the data, which is often done for convenience, especially to facilitate more convenient subsequent processing. The shape of the region of support will define the overall shape of the IPR.[17] Because of the limited region of support, the IPR thus generated will only be an approximate rendering of the actual impulse target itself. That is, simply limiting the region of support will itself limit the fidelity of the rendering of the impulse target.

Nevertheless, Eq. (10) essentially implements a matched filter (more specifically a correlator) against a spectrally constrained set of complex sinusoids.

Rectangular Region of Support

We will examine basic IPR characteristics by considering the simplifying assumption of a rectangular region of support. Accordingly, we now define the rectangular region of support as

$$A\left(k_x, k_y\right) = \text{rect}\left(\frac{k_x - k_{x0}}{K_x}\right) \text{rect}\left(\frac{k_y - k_{y0}}{K_y}\right), \tag{11}$$

where

$$\begin{aligned} k_{x0}, k_{y0} &= \text{k-space coordinate of center of region of support,} \\ K_x, K_y &= \text{k-space span or width of region of support,} \end{aligned} \tag{12}$$

and

$$\text{rect}(z) = \begin{cases} 1 & |z| \le 1/2 \\ 0 & \text{else} \end{cases}. \tag{13}$$

For this rectangular region of support, we may calculate the 2-D IPR in closed-form as

$$W_2(x - s_x, y - s_y) = \left\{ \begin{array}{l} \left(\dfrac{K_x K_y}{(2\pi)^2} \right) e^{+j\left(k_{x0}(x - s_x) + k_{y0}(y - s_y)\right)} \\ \times \text{sinc}\left(\dfrac{K_x}{2\pi}(x - s_x) \right) \text{sinc}\left(\dfrac{K_y}{2\pi}(y - s_y) \right) \end{array} \right\}, \tag{14}$$

where

$$\text{sinc}(z) = \sin(\pi z)/\pi z\,. \tag{15}$$

From this we observe the following.

- The IPR is most definitely a 2-D function. It generally extends in all directions, just more so in some directions than others, but definitely in all directions.
- This IPR peaks where x, y coordinates are at the location of the impulse target, s_x, s_y.

  The immediate region around this peak is characterized by a lobe, which we call the mainlobe of the IPR.
- The nominal width of the mainlobe in cardinal directions that are the principal axes of the IPR, are given by

  $$\rho_x = 2\pi/K_x \text{, and}$$
  $$\rho_y = 2\pi/K_y\,. \tag{16}$$

  These nominal widths are referred to as the nominal resolution of the IPR in these principal axis directions. Consequently, the span of the region of support in various directions will define, or at least limit the resolution achievable with the corresponding radar data.

  For the sinc functions of Eq. (14), although the nominal mainlobe widths are as given in Eq. (16), the resolution in terms of the half-power mainlobe widths are actually approximately 0.886 times these numbers. This is just a characteristic of the sinc function.
- With respect to the IPR, as distance increases from the mainlobe peak, most notably in the cardinal directions, additional lobes manifest but with diminishing magnitude. These are called "sidelobes." They are essentially grating lobes manifesting as a ringing that are caused by the sharp edges of the region of support. They are exacerbated by long straight edges in the region of support. Sidelobes will be generated in a direction normal to the edges of $A(k_x, k_y)$.[18]

For the sinc functions in Eq. (14), the first sidelobes are the largest and only 13 dB below the mainlobe peak, and fall off in magnitude as approximately the inverse of the distance from the mainlobe peak. The relative magnitude of the largest sidelobe with respect to the IPR mainlobe peak is termed "Peak Sidelobe Ratio" (PSLR).

- The collection of sidelobes is sometimes referred to as "spectral leakage" as they constitute energy that has essentially escaped the mainlobe. The fraction of total IPR energy resident in all sidelobes is termed "Integrated Sidelobe Ratio" (ISLR).

  For the sinc functions in Eq. (14), each sinc function is responsible for an ISLR of about −10 dBc, making the total ISLR for the 2-D IPR about −7 dBc.

The above analysis assumed a rectangular region of support. This made it somewhat easy to introduce the observations above. Now we offer some comments about rectangular regions of support generally.

- For other non-rectangular shapes of the wavenumber region of support, we will definitely alter the sidelobe structure of the IPR.
- In some quarters, it is desired that this region of support in fact be rectangular, although the specific reasons for this in a particular application are not always clear or justified. We opine that even non-rectangular regions of support are quite useable for a large number of applications, without any ill effects.‡
- Rectangular regions of support are not natural to SAR data collections. Commonly, after data collection, the k-space is cropped to a rectangular region using signal processing, and usually also resampled to a rectangular grid therein. This cropping sacrifices both Signal-to-Noise Ratio (SNR) and resolution to some degree. However, the resulting often simplified processing required and more predictable sidelobe structure are sometimes considered a good trade, but not always by everybody.
- Sometimes, SAR data collection strategies can be modulated to collect the initial phase history data to a k-space region of support that is closer to (albeit not exactly to) a rectangular region of support, thereby minimizing any further cropping. This can be done with real-time motion compensation with waveform manipulation.[19,20]
- Some SAR image formation processing algorithms are more tolerant than others to non-rectangular regions of support. For example, Backprojection algorithms usually don't care.[21] Common implementations of the Polar Format Algorithm (PFA) often preprocess the data to a rectangular region of support before actual image formation processing.[22]
- For other non-rectangular shapes of the wavenumber region of support, we may need to do a deeper dive into what exactly is meant by "resolution." Such a study (of what might be meant by "resolution" generally) is a fascinating area in and of itself that could easily be a dissertation in its own right. We provide some additional comments in Appendix A.

‡ Without elaboration, we stipulate that perfectly fine and useable SAR images are routinely generated by operational systems that employ other than rectangular regions of support.

Sidelobe Mitigation

As previously mentioned, for the rectangular region of support defined by Eq. (11), the corresponding sinc functions in Eq. (14) exhibit first sidelobes that are only 13 dB below the mainlobe peak, and an ISLR for the 2-D IPR of about −7 dBc. Furthermore, the sidelobes fall in magnitude as approximately the inverse of the distance from the mainlobe peak, albeit in the cardinal directions. This is often considered inadequate in that we frequently desire sidelobe levels considerably lower than this, and perhaps falling off at a faster rate with distance from the mainlobe peak. Recall that sidelobes are energy that has leaked away from the IPR mainlobe, and are no longer adequately local to the target impulse location. In doing so, they may obscure weaker targets elsewhere in the target scene.

The customary signal processing technique for reducing sidelobes in an IPR is to employ window taper functions.[18]

Recall that we heretofore stipulated Eq. (9), that is, that the wavenumber region of support had hard edges. It is these hard edges that generated sidelobes. By softening, i.e., tapering the edges of the region of support, we can attenuate sidelobes at the expense of somewhat broadening the IPR mainlobe response. This is usually considered a good trade.

The usual application of window taper functions is to apply them as orthogonal 1-D window-taper functions to the 2-D data array. For a rectangular region of support, Eq. (11) now becomes

$$A\left(k_x, k_y\right) = w_x\left(\frac{k_x - k_{x0}}{K_x}\right) w_y\left(\frac{k_y - k_{y0}}{K_y}\right), \tag{17}$$

where

$$w_x(z), w_y(z) = \text{1-D window taper functions.} \tag{18}$$

These window taper functions are defined over the interval $[-1/2\,,1/2]$, otherwise considered zero outside this interval. Within this interval they are typically real-valued, and we shall presume so here going forward. Furthermore, there is no requirement that $w_x(z)$ and $w_y(z)$ be the same window taper function, although for SAR images they often are.

We offer several comments.

- The nominal width of the mainlobe in cardinal directions that are the principal axes of the IPR, i.e., corresponding resolutions, are now given by

$$\begin{aligned} \rho_x &= 2\pi a_{wx}/K_x \text{ , and} \\ \rho_y &= 2\pi a_{wy}/K_y \text{ ,} \end{aligned} \tag{19}$$

  where

$$a_{wx}, a_{wy} = \text{IPR mainlobe broadening in the respective cardinal directions.} \tag{20}$$

- In addition, the desired effect of employing a window taper function is a reduction in PSLR, and a reduction to ISLR. This is after all what we are generally after.
- Since the window taper function is essentially another filter concatenated with the matched filter processing to form the SAR image, the combination represents an overall slightly detuned matched filter with the result of further slightly reducing the achievable SNR. This SNR loss is usually on the order of a dB or so for window functions in any individual dimension, and is considered quite tolerable.

As an example, a common, albeit nowhere near exclusive, window taper function used for microwave SAR processing is the Taylor Window, with −35 dB PSLR and parameter nbar = 4. This is a 1-D function usually applied in both orthogonal directions to the 2-D data array. This 1-D function is illustrated in Figure 2.[18]

If we use the window taper function of Figure 2 in both orthogonal directions, then we can expect for the overall 2-D IPR

$$\begin{aligned} &a_{wx}, a_{wy} \approx 1.1841, \\ &PSL \approx -35\,\text{dBc}, \\ &ISLR \approx -24\ \text{dBc, and} \\ &L_{SP} \approx 1.8\ \text{dB (total signal processing SNR losses).} \end{aligned} \tag{21}$$

Note that ISLR and total signal processing loss L_{SP} represent the collective parameters from using the same Taylor window in both dimensions.

We offer some additional comments.

- We emphasize that the 2-D data array onto which the orthogonal 1-D window taper functions are applied need not necessarily represent specifically a rectangular region of support in the wavenumber domain.

  We offer without elaboration an example that the window taper functions can be applied to raw data prior to resampling to within a circumscribed rectangle in k-space. Another example is using window taper functions during SAR image formation using Backprojection processing.
- We have tacitly assumed that the wavenumber region of support is contiguous and fully filled, i.e., no gaps or holes. This may not always be true, especially when regions in k-space are excised to accommodate, say, spectral restrictions, or interference mitigation. This will naturally impact IPR characteristics.[23,24]

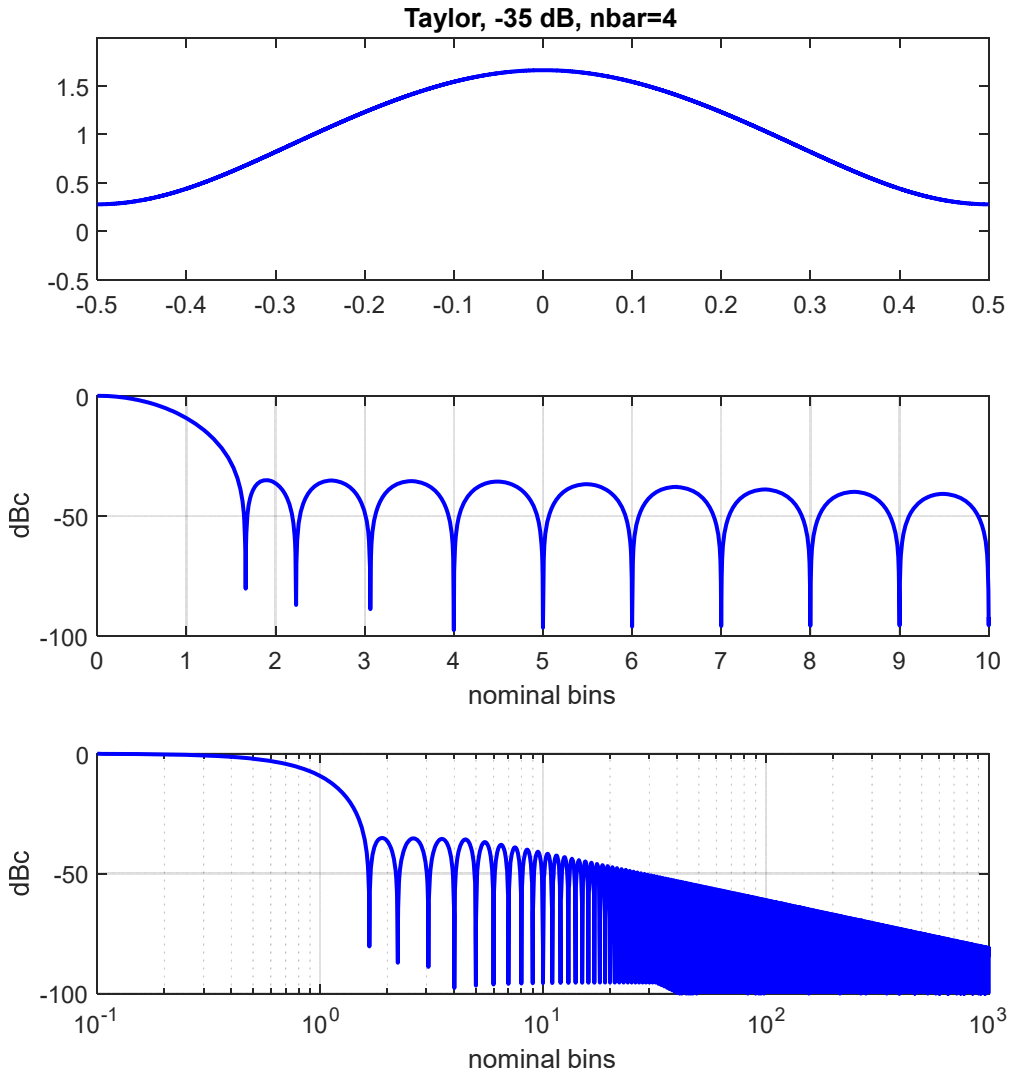

WINDOW SPECTRUM CHARACTERISTICS

half-power bandwidth = 1.1841 (normalized to 1/T)
-3 dB bandwidth = 1.1821 (normalized to 1/T)
-18 dB bandwidth = 2.611 (normalized to 1/T)
noise bandwidth = 1.2343 (normalized to 1/T)
SNR loss = 0.914 dB
first null = 1.6641 (normalized to 1/T)
PSLR = -35.1672 dBc
ISLR = -27.1388 dBc from first null outward

Figure 2. Window Taper function for –35 dB Taylor window, nbar=4. The top plot is the taper function itself, and the bottom two plots are the 1-D IPR from mainlobe center outward.

Related Issues

We now offer some gratuitous comments related to the previous analysis, usually without further elaboration.

- The portion of the 3-D world that makes up a SAR scene implies that the overall wavenumber domain for a scene is 3-D as well. This begs the question "What does this mean for the k-space of an image?" A common assumption for SAR is that the target scene of interest is a flat surface, i.e., a surface of uniform height at $s_z = 0$. This suggests that the z-dimension (height) can be modelled as an impulse with respect to this third dimension. This in turn implies that the 3-D k-space exhibits constant values in the k_z direction. This further in turn allows us to project values at any k_z location into the $k_z = 0$ plane. Thereafter, we can restrict our attention to just this 2-D planar surface of the overall k-space. Essentially, we have advantageously thereby reduced the 3-D problem into a 2-D problem. The price we pay is some degradation of actual scatterers that are not in fact in the presumed flat surface for the SAR image. This manifests as a geometric distortion known as image layover, and Height-of-Focus issues.[25]
- Not all image locations, i.e., locations in an image for an impulse target, will exhibit the same region of support. That is, the precise definition of the region of support may itself be spatially variant. This can confound some image processing techniques such as autofocus for some images created with certain processing algorithms such as Backprojection.[21]
- Nonlinear techniques do exist to mitigate IPR sidelobes, some even with the benefit of not broadening the IPR mainlobe. These are generally referred to as sidelobe apodization algorithms.[26,27] These are beyond the scope of this report.
- Other techniques have also been proposed that allow finer resolution than what Eq. (16) suggests, and more generally IPR improvement in some sense. Many of these make assumptions about SAR image scene content, and involve some degree of k-space extrapolation of the wavenumber region of support. These often fall within the general topic of "Superresolution."

  We caution the reader to draw distinction between renderings that are "more accurate" vs. "look nicer" vs. "more useful for subsequent exploitation." These are not all the same.[28]
- While the –35 dB Taylor window taper function described in Figure 2 is somewhat common for SAR processing, it is not necessarily adequate for other modes that make similar range-Doppler maps during the course of their processing. For example, Moving Target Indicator (MTI) modes often require more substantial sidelobe suppression than for SAR. This necessitates other window taper functions for those modes.

2.2 System Linearity and Signal Distortions

The previous section discussed the wavenumber region of support, especially how its boundaries impacted the IPR. We also discussed tapering the edges of this region with real-valued window functions to suppress sidelobes, but at the expense of coarser resolution and SNR reduction.

Within the region of support, apart from any tapering for sidelobe control, we tacitly assumed perfect replication of the wavenumber function for an impulse, i.e., unit modulus and linear phase rotation consistent with Eq. (8). Any departure from this will impact the overall IPR in addition to the limited wavenumber region of support and any tapering. Since SAR images often may exhibit 100 dB or more of dynamic range, even seemingly small perturbations in the wavenumber function may be noticeable, and perhaps become objectionable.

We begin the following discussion by noting that there are a whole lot of ways to screw up a SAR image. Regardless of what quality means to you, there are many things that have to be done correctly to achieve the desired utility.

Window taper functions notwithstanding, we now discuss sources of IPR distortion due to non-ideal variations of either or both amplitude and phase within the wavenumber region of support. Basically, anything that generally affects the phase or amplitude, mainly by causing fluctuations or modulations, within the wavenumber region of support will adversely affect the IPR. This will likely be first noticed in the sidelobe structure of the IPR, but ultimately also perhaps in the IPR mainlobe. Some anomalies will affect IPR sidelobes more in range, and some more in cross-range, and some in both. Component and circuit impact on IPR is discussed in an earlier report.[29]

We will divide signal distortions resulting in IPR degradation into two main classes.

1. Channel Gain Nonlinearities
2. Signal Modulations

We might argue on occasion whether a particular degradation is wholly one or the other. We will discuss here sources of distortions and IPR degradation mostly in a qualitative sense, reserving recommendations for quantitative measures for later.

2.2.1 Channel Gain Nonlinearities

It is well-known that a non-linear function applied to a sinusoid will generate harmonics. This is in fact how mixers and multipliers are implemented with circuit elements. However, when a signal channel is desired to be linear and distortionless, any nonlinear circuit elements will interfere with signal transmission and adulterate the result. We generally don't want this.

Receiver (RX) Channel Dynamic Range

Most circuit elements, but especially active components, have limits on how strong a signal they can pass. This limits the effective dynamic range of a circuit. We desire this dynamic range restriction to be well-understood and stable. Usual RX circuit design, and subsequent operation, will allow acceptably linear operation to some maximum signal level, and avoid signal levels

greater than this where signals become unacceptably nonlinear or distorted. This maximum signal level typically corresponds to the maximum signal level that can be processed by the receiver's Analog-to-Digital Converter (ADC), rendering the ADC as the dynamic range chokepoint. This predictable behavior is generally desired.

ADC Nonlinearities

The ADC samples and quantizes the input analog signal. It is generally expected that the ADC quantizes in predictable uniform step sizes. To the degree that this is not absolutely true, the ADC imposes its own nonlinearities upon the digitized signal. Especially with the large SNR gains due to SAR signal processing, the effects of these nonlinearities may become quite evident in the data, and ultimately in the SAR image. This is explored in detail in an earlier report.[30]

I/Q Imbalance

Radar data is usually down-converted to baseband for subsequent processing. The need to distinguish positive frequencies from negative frequencies usually requires baseband data to be complex-valued, with real and imaginary components, often referred to as In-phase (I) and Quadrature-phase (Q) data, collectively called I/Q data. The I and Q channels must be accurately and precisely represented in both amplitude and phase. They need to be properly and adequately balanced. This can be problematic, and is explored in detail in an earlier report.[31]

Transmit (TX) Channel Gain Nonlinearity

The TX channel begins with waveform generation and continues through to the antenna. The final TX power amplifier is usually driven into compression to maximize its power output. This has two principal effects. The first is there is little need for the intervening circuits to remain linear with respect to amplitude, since the final amplifier destroys this linearity anyway.[§] The second is that any amplitude characteristics of the generated waveform will thereby also be suppressed, pushing us to use constant modulus waveforms, or equivalent. This means limiting desired waveform modulations to phase modulations (or perhaps frequency modulations).

Nevertheless, it remains prudent to assess how nonlinearities in the TX channel may generate modulation and intermodulation products that then mix and multiply in subsequent nonlinearities, thereby generating problematic spurious signals that are then transmitted and received and ultimately rendered as artifacts in the SAR image. This includes nonlinear behavior of any Digital-to-Analog Converter (DAC) employed for signal generation.

In a similar manner, if a Local Oscillator (LO) signal is similarly generated, and then mixed with the RX signal for down-conversion, such spurious signals via the LO may also modulate the RX signal to an undesired effect, perturbing the ultimate IPR.

[§] We caveat this statement to note that sometimes we might desire the radar's final power amplifer to not operate at full power. Power might then be reduced by reducing input signal drive levels, which in turn might lessen the degree to which signals are compressed in amplitude at the amplifer output, perhaps even moving back to linear gain operation. This implies that signal gain by the amplifier is drive-level dependent, and the ability to program a drive level for a precise power output will require calibrating the gain function.

2.2.2 Signal Modulations

Apart from data tapering, we expect an impulse target to generate data within the wavenumber region of support that is uniform amplitude, and linear phase, as a function of wavenumber coordinates. Any fluctuations in amplitude or fluctuations in phase represent modulations to the wavenumber domain data that will ultimately impact IPR. Such modulations are equivalent to Amplitude Modulation (AM) and Phase Modulation (PM) in communication systems.[32] SAR IPR sidelobes are equivalent to communication signal sidebands.

Modulations may occur within a single pulse's echo data record, or across pulses, or both. Recall that the intra-pulse dimension will normally correspond to the range IPR, and the inter-pulse dimension will generally correspond to the cross-range or azimuth IPR.

We may generally classify modulations into

1. Low-frequency modulations – These are modulations that generally limit their effect to the mainlobe of the IPR, usually broadening the mainlobe. Such modulations, whether amplitude or phase, resemble less than half a cycle of a sinusoid. A quadratic function fits this model.
2. High-frequency modulations – These are modulations that manifest in noticeably raised sidelobes in the IPR. Such modulations, whether amplitude or phase, have features that resemble multiple cycles of a sinusoid.

The effects on IPR of various phase and amplitude error characteristics are discussed in a previous report.[17] We repeat some of them here in Figure 3 to illustrate for 1-D functions. While the IPR depends on the nature of the amplitude and phase modulations within the wavenumber region of support, it is important to realize that the origin of modulations in the wavenumber region of support might be well upstream from the point where the signal becomes relevant data. In fact, both amplitude and phase modulations may begin as something else. For example, it is well-known that non-linear components can convert AM signals into PM signals.[33] Other nonlinear components and circuits can convert PM signals into AM signals. Nevertheless, the IPR still depends on how these modulations manifest in the wavenumber region of support.[**]

We further observe that radar calculates range from a presumed radar location using echo time delay which usually presumes a well-behaved transmission medium (atmosphere) with known constant propagation velocity and minimal refraction, with time delay in turn calculated by counting clock cycles, which are presumed to be uniform and constant in frequency. None of these presumptions are strictly true. Errors in any of these presumptions will degrade the SAR image IPR.

We now discuss several sources of modulations and distortions that will ultimately affect SAR image IPR.

[**] It is sometimes useful to ascertain whether a particular IPR degradation is due to amplitude versus phase modulations. These can sometimes be distinguished by separating magnitude from phase data in k-space, and substituting perfect phase or magnitude respectively, before reprocessing into an IPR. These might be referred to as "magnitude IPR" or "phase IPR" respectively.

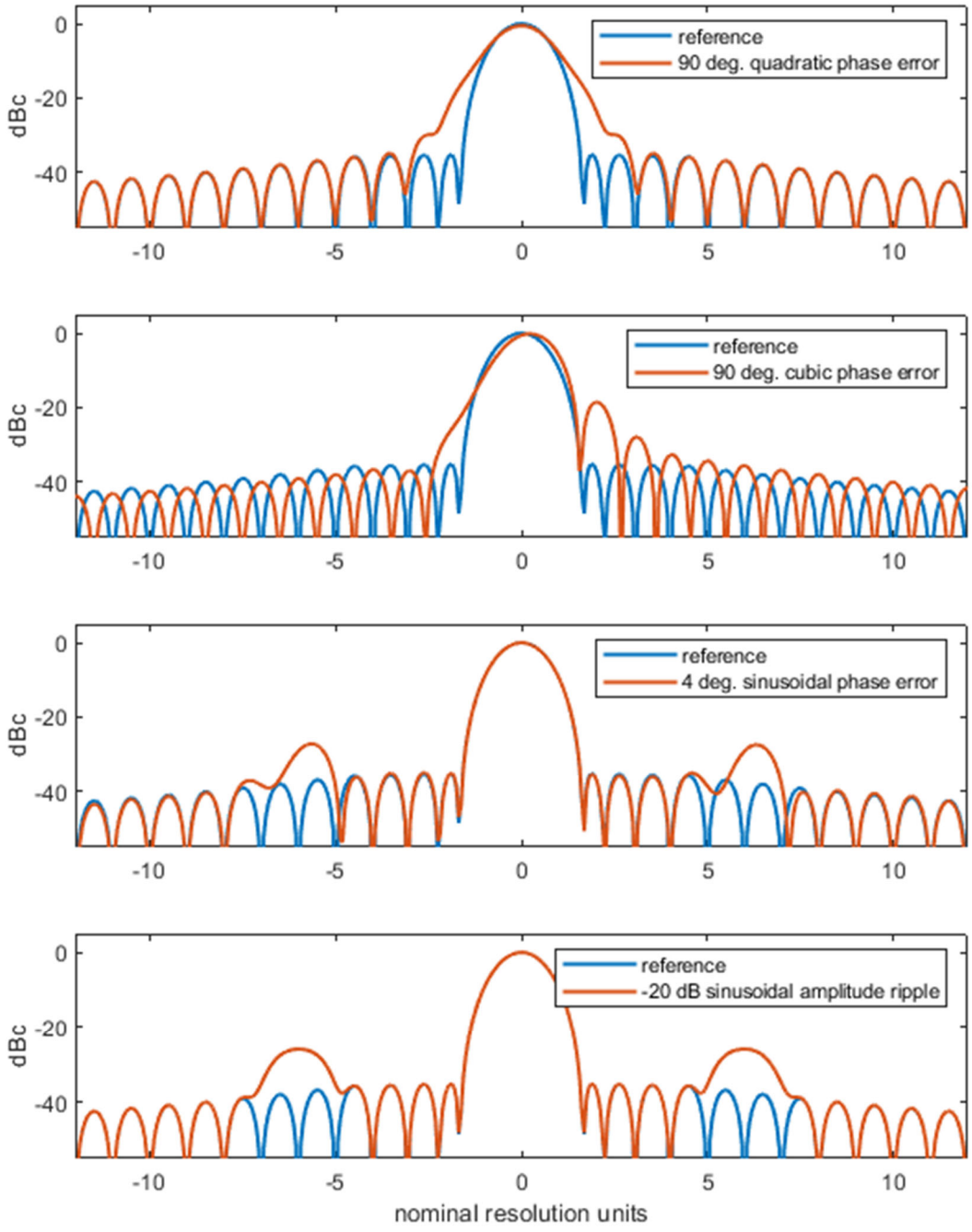

Figure 3. Example IPR degradations due to phase and amplitude errors. Reference plots are for –35 dB Taylor window taper function displayed in Figure 2. Nominal resolution is with respect to untapered, or uniform window taper function.

2.2.2.1 Single Pulse Modulations

Here we address several sources of distortions evident even for a single pulse's radar echo.

The RX Channel Modulations

We desire the radar RX channel to be distortionless, that is, providing only constant gain and linear-phase as ultimately represented in the corresponding direction for the wavenumber function for a point target. We note that some waveforms, notably the Linear-Frequency-Modulated (LFM) chirp, will essentially transfer channel frequency-dependent distortions directly to the wavenumber domain as wavenumber-dependent distortions, by their nature of corresponding instantaneous frequency with time delay.[34] This is true for both phase nonlinearities as well as passband ripple.[35,36]

Return Loss

Return loss is the manifestation of additional delayed echo energy, observed as a ghost signal offset to a farther range from the principal desired echo return. For a point target, it manifests usually as a single sidelobe delayed in time from the mainlobe response. It is generated by transmission line phenomena resulting from signal path impedance mismatches, and most evident with longer signal paths, such as with microwave cables and their connectors.

Analysis of a return loss echo signal shows that it can be decomposed into precisely balanced sinusoidal amplitude and phase modulations. Note that compensating one of either the amplitude or phase modulation, and not the other, will cause the one-sided sidelobe response to now manifest as a two-sided response.[††]

Doppler Tolerance

When the echo range/delay between radar and point target is changing during a single pulse's echo time, then the echo response will exhibit a Doppler shift, in addition to a pulse-to-pulse phase shift that is the more exploited effect. Nevertheless, with sufficient relative line-of-sight velocity, the echo of even a single pulse will manifest a frequency shift. More properly, the Doppler effect is a distortion that manifests as a time scaling, either a dilation or compression depending on increasing or decreasing range with time. From Fourier analysis, a time scaling is equivalent to a frequency scaling with inverse proportionality. This means that a Doppler shift is really a Doppler scaling, that it, a frequency-dependent frequency shift.

Since SAR processing essentially implements matched filter processing, ignoring this distortion will manifest as a degradation of the IPR. The severity of the IPR degradation will depend on the nature of the waveform used by the radar, specifically how well it can tolerate intra-pulse Doppler scaling. Some waveforms are more tolerant than others.

[††] Without elaboration, we state that this fact can sometimes be used to distinguish between a TX channel cable return loss issue from a RX channel cable return loss issue. This is especially true when an extended TX channel cable precedes the final power amplifier which is often operated in compression.

The TX Channel Modulations

If the TX waveform were intended to preserve amplitude modulations as well as phase modulations of the waveform generator, then all the channel modulation comments made for the RX channel would also apply here. However, this is usually not the case.

As previously discussed, more typically, the TX waveform is compressed in amplitude by the radar's final power amplifier to maximize the transmitted peak power. This means that there is no real need to maintain any channel linearity with respect to amplitude modulations ahead of the final power amplifiers, either. Consequently, radar systems tend to employ phase or frequency modulations rather than purposeful amplitude modulations.

Nevertheless, we do desire for the TX channel to maintain accurate and precise phase modulations, that is, to not detrimentally distort the phase of the waveform. We desire components to maintain phase linearity as a function of frequency. Where frequency multipliers are used, we desire perfect phase multiplication for all frequencies, and similarly for mixers.

We digress for a moment to note that what really needs to remain phase-linear is the entire signal path beginning with waveform generation, and perhaps ending with sampled data in the receiver, although this somewhat depends on RX channel architecture. If phase distortions are stable, then the opportunity exists to pre-distort the TX waveform to counter or compensate for later distortions. In communication systems this is often referred to as "channel equalization." Applying frequency-dependent phase predistortions to linearize the overall channel is particularly easy to do with frequency-modulated waveforms, such as the LFM chirp.[37,38]

Nevertheless, we summarize that TX channel nonlinearities can also manifest as undesired modulations in the RX data, and impact IPR accordingly.

Signal Dispersion

The signal path from TX waveform synthesis to RX data sampling may contain elements that exhibit dispersion, that is, frequency-dependent delay. This sort of distortion is natural to some components such as waveguides, as well as to signal propagation mediums such as the ionosphere.

In a similar manner, Active Electronically Steered Array (AESA) antennas that employ phase shifters to steer wideband signals instead of True Time-Delay (TTD) elements will similarly affect the IPR from a spatial point target.

2.2.2.2 Pulse-to-Pulse Stability

Here we address several sources of distortions evident across multiple pulses' echoes.

Residual Motion Errors and Autofocus

SAR imaging assumes that the scene being imaged is static, i.e., nothing is moving. In addition, the scene is usually assumed to be flat. Furthermore, the synthetic aperture, defined as the diverse set of locations from which the pulses are emitted and echo soundings are collected, are perfectly known to the data collection process and image formation algorithm. It is the task of the motion measurement subsystem, also known as the "navigator," to provide the radar motion data necessary to properly collect and process the data.

There are limits to the accuracy and precision of motion estimates by the navigator.[39] Errors with respect to the true collection geometry will manifest as range errors and associated echo delay errors, which are often modelled as phase errors. Such errors often vary from one pulse to the next, and may exhibit nonlinear characteristics, resulting in significant IPR degradation.[40] In fact, for fine-resolution SAR imaging, this is often the dominant source of IPR degradation.

The usual mitigation scheme for residual IPR degradation due to unmeasured motion errors is to estimate the phase/delay error from the data itself, and then deconvolve this from the data set. This process is called "autofocus." A variety of autofocus algorithms exist, with Phase-Gradient Autofocus (PGA) having become one of the more popular ones.[41] This topic is extensively treated in the published literature. In general, autofocus processing of SAR images works quite well, significantly improving the IPR rendering of point targets.

Atmospheric Effects

While motion measurement errors can indeed cause phase/delay errors in the radar's collected data, all the radar really sees are the phase/delay errors themselves. There are other error sources to cause similar phase/delay errors, notably the atmosphere itself. Recall that the radar infers ranges from echo time delay, assuming a constant velocity of signal propagation, and often something close to free space velocity of signal propagation. This may be overly optimistic. The atmosphere is neither free space, nor is it even homogeneous, in any direction. The result is often phase/delay errors that are indistinguishable from apparent motion errors. In fact, these phase/delay errors might even be different in different parts of the SAR image, i.e., spatially variant phase/delay errors, that result in spatially variant IPR degradation.[42]

Pulse Modulation Fluctuations

A generalization of the previous paragraphs is that any pulse modulation that varies from pulse to pulse offers the opportunity to in turn cause pulse-to-pulse modulations that degrade the IPR in that dimension, even if the individual pulses' modulations are perfectly known. This is more of a problem with some waveforms than others, especially with random or chaotic waveforms.[43]

Time-Base Noise

Recall that a radar estimates time delay from essentially counting its internal clock cycles, assuming that those clock cycles are uniform and at a constant frequency. They are in fact not so, or at least not perfectly so. Random fluctuations in the basic radar time base will appear as fluctuations in measured delay times, and hence fluctuations in radar calculated range, and hence in radar echo phase/delay. These time-base fluctuations are sometimes called clock jitter, and perhaps more popularly known as phase noise.[44,45]

To be sure, the manifestation of phase noise in a SAR image is usually a low-level effect, but may still be noticeable and objectionable. Phase noise will generate a low level IPR sidelobe floor typically in the azimuth direction, but sometimes in a band, associated with some bright target scatterer in the image. The high dynamic range nature of SAR images might still often make these low-level sidelobes visible. Anecdotally, we often desire the phase noise floor in the SAR image be no higher than −70 dBc or so.

Since the underlying clock source for a radar's Stable Local Oscillator (STALO) frequency source is typically a single master oscillator employing a piezoelectric crystal, the piezoelectric nature of the crystal also makes the phase noise exacerbated by crystal mechanical vibrations.

While the master oscillator may be an unavoidable source of phase noise, and is often chosen to be a low-phase-noise device, other components may add significantly to overall system phase noise. One class of components that do so, and therefore must be employed with great care and some trepidation, is the Phase-Locked Loop (PLL).[‡‡] These are also discussed in an earlier report.[44]

Aliased Clutter

Heretofore we have been discussing perturbations to a point target response that we want to observe. We now discuss the related issue of not adequately suppressing a point target that we don't want to observe. So, while not an IPR issue, per se, the pulsed nature of pulse-Doppler radar systems brings all the attributes of sampled-data systems to our data collection and processing. This includes aliasing of other physical locations into our SAR image, typically in the cross-range dimension, although under the right circumstances also in the range dimension.[46] While we expect the radar's antenna beam to function as an anti-aliasing filter for SAR, we remain mindful that there are limits to the antenna's ability to attenuate signals in directions outside of its mainbeam. Target responses will still often manifest through the antenna beam sidelobes, attenuated but not eliminated.

Careful selection of radar Pulse Repetition Frequency (PRF) along with possibly Doppler filtering (e.g., presumming) can reduce the impact of aliasing, but not eliminate it. Anecdotally, we often choose SAR operating parameters to suppress aliased energy by at least 40 dB or so. In spite of this, it is not uncommon to find aliased artifacts in SAR images, both in range and in cross-range.

[‡‡] Without elaboration, we stipulate that operational radars exist that have undergone costly redesign due to excessive phase noise from careless employment of PLL devices in their STALO module.

Target Motion

The presumption for SAR imaging is that the target scene is a rigid body, and static. Anything that moves during the synthetic aperture data collection is violating the basic assumptions, and hence will manifest with anomalous rendering in the SAR image. Translations in the line-of-sight range direction will generally cause a cross-range shift in energy location, and a cross-range motion will cause a cross-range smearing of the moving target echo energy. Motion may be due to wind-blown vegetation, moving vehicles, walking people or animals, turning wind turbines, rotating antennas, air-conditioning fans, vibrating structures, and anything else that isn't standing perfectly still. Any of these will make a SAR image look uglier, by rendering smeared foliage or seemingly disembodied streaks. An example of the effects of wind-blown tree foliage is shown in Figure 4.

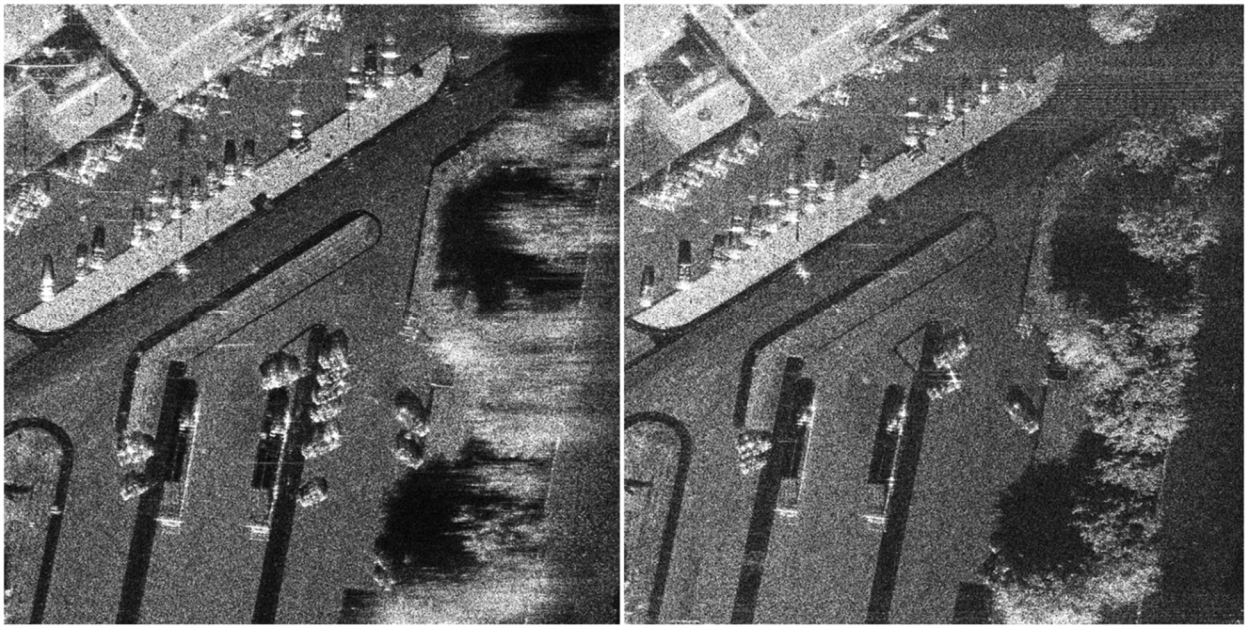

Figure 4. Notice that the wind-blown tree foliage in the left image is smeared compared to the same scene imaged on a calm day in the right image.

While target scene motion has an effect on SAR image quality, there is very little to prevent it short of controlling the contents of the scene being imaged. Consequently, there is really no way to include limits due to this in any image quality specification.

We do note that a still current area of research is the ability to 'focus' moving vehicles and perhaps correct their physical location with respect to the underlying stationary clutter scene. A paper by Garren is representative.[47]

Another area of still current research is to detect and characterize vibrating targets. A paper by Campbell, et al., is representative.[48]

Multipath Effects

The SAR imaging process generally makes use of the Born approximation.[49]

In a complex scattering environment, the echo energy from a particular scatterer is due to the total field, which includes the un-reflected incident field as well as all fields that were previously scattered in some manner by other elements in the target scene. Image reconstruction under these circumstances is generally intractable. Consequently, we simplify the image reconstruction problem to only consider the un-reflected incident field. This is the Born approximation.

However, the Born approximation is just an approximation, and using it will result in errors during image reconstruction, sometimes severe. These errors may result in anomalies in the SAR image such as visible artifacts and false features, thereby diminishing SAR image fidelity.[§§]

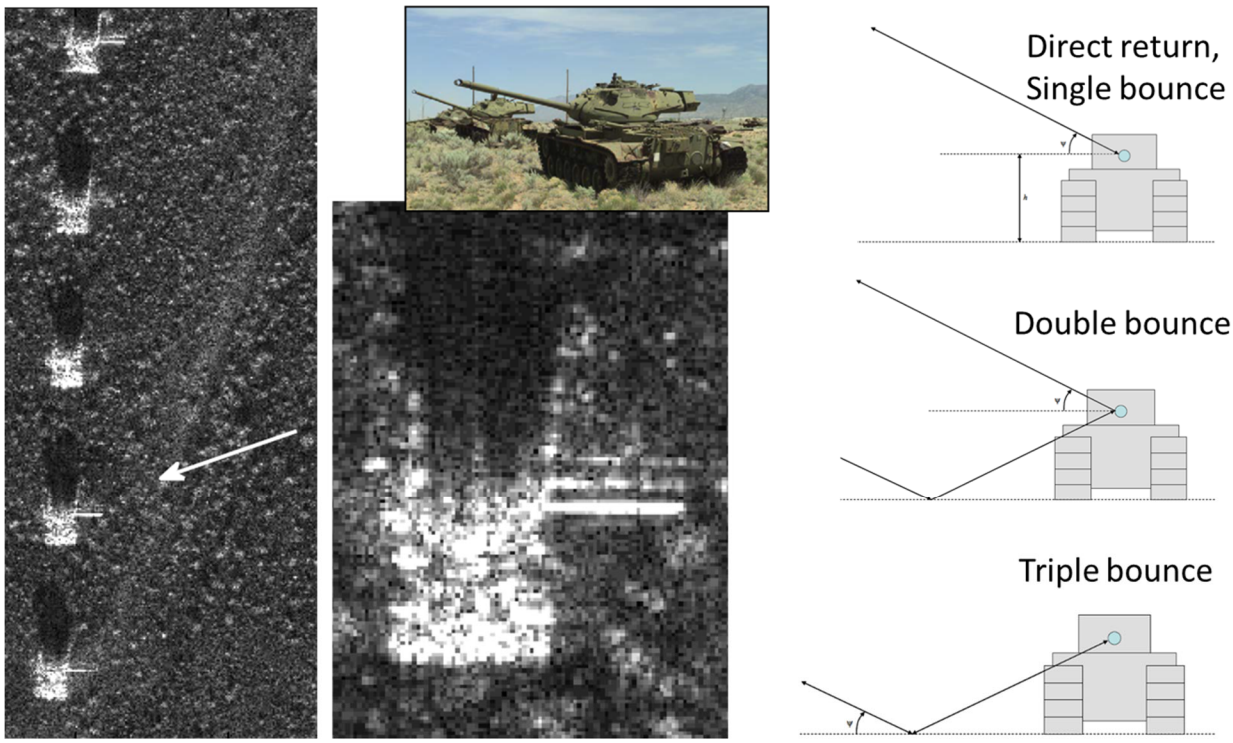

Figure 5. Example of multipath where the SAR image of a tank exhibits three cannon barrels whereas ground truth shows only a single barrel. Careful analysis of imaging geometry shows that the apparent three barrels are due to the direct return, a multipath single bounce from the ground, and a multipath double bounce from the ground.

As with target scene motion, there is very little to prevent it in the target scene and consequently there is really no way to include limits due to this in any image quality specification. Attempts have been made to exploit multipath effects, with a paper by Setlur, et al., being representative.[50]

[§§] The word "artifact" is often applied to seemingly false echo energy that we cannot or don't want to explain. It is often used in place of the more embarrassing "I don't really know what that is."

2.3 IPR Quality Measures

In the previous sections we have discussed IPR perturbations caused by any of a number of anomalies in the overall signal channel. Many of these offer cumulative degradations to the IPR. Furthermore, their impact on a point target tracks the actual point target signal level. Consequently, they are described as being "multiplicative" in nature, as opposed to additive.

IPR Limits

Nevertheless, it remains true that a common measure of goodness of the ability of a radar to represent targets is the IPR. Consequently, it seems reasonable to specify limits on the degradation of SAR image IPR as a system design specification and evaluation measure. At a minimum, limits on IPR principal cuts at cardinal angles of range and cross-range can be specified and evaluated.

A reasonable set of specification criteria for principal IPR cuts might be[29]

1. limit measured IPR characteristics to have a mainlobe with half-power width no wider than 10% greater than that of the ideal window taper function IPR response,
2. limit IPR −18 dBc mainlobe width to no wider than three times that of the ideal window taper response's half-power width,
3. limit IPR sidelobes to be no greater than about 10 dB above the sidelobes for the ideal window taper function IPR response, with some additional allowance for near-in sidelobes, and also 10 dB above the desired noise floor due to time-base phase-noise desired limits.

For the −35 dB Taylor window taper function of Figure 2 we might choose an IPR specification for a principal cut to be

$$\text{IPR\_limit}_{dBc} = \begin{cases} -3 & u = 0.55 \\ (e_0 - e_1)\left(1 - \dfrac{\log_{10}(u/u_0)}{\log_{10}(u_1/u_0)}\right)^m + e_1 & u_0 \le u < u_1 \\ (e_2 - e_1)\left(1 - \dfrac{\log_{10}(u/u_1)}{\log_{10}(u_2/u_1)}\right) + e_1 & u_1 \le u < u_2 \\ e_2 & u_2 \le u \end{cases}, \tag{22}$$

where the breakpoints are defined to be

$$\begin{aligned} &u_0, e_0 = 1.5, -18, \\ &u_1, e_1 = 7, -30, \\ &u_2, e_2 = 235, -60, \text{ and} \\ &m = 2. \end{aligned} \tag{23}$$

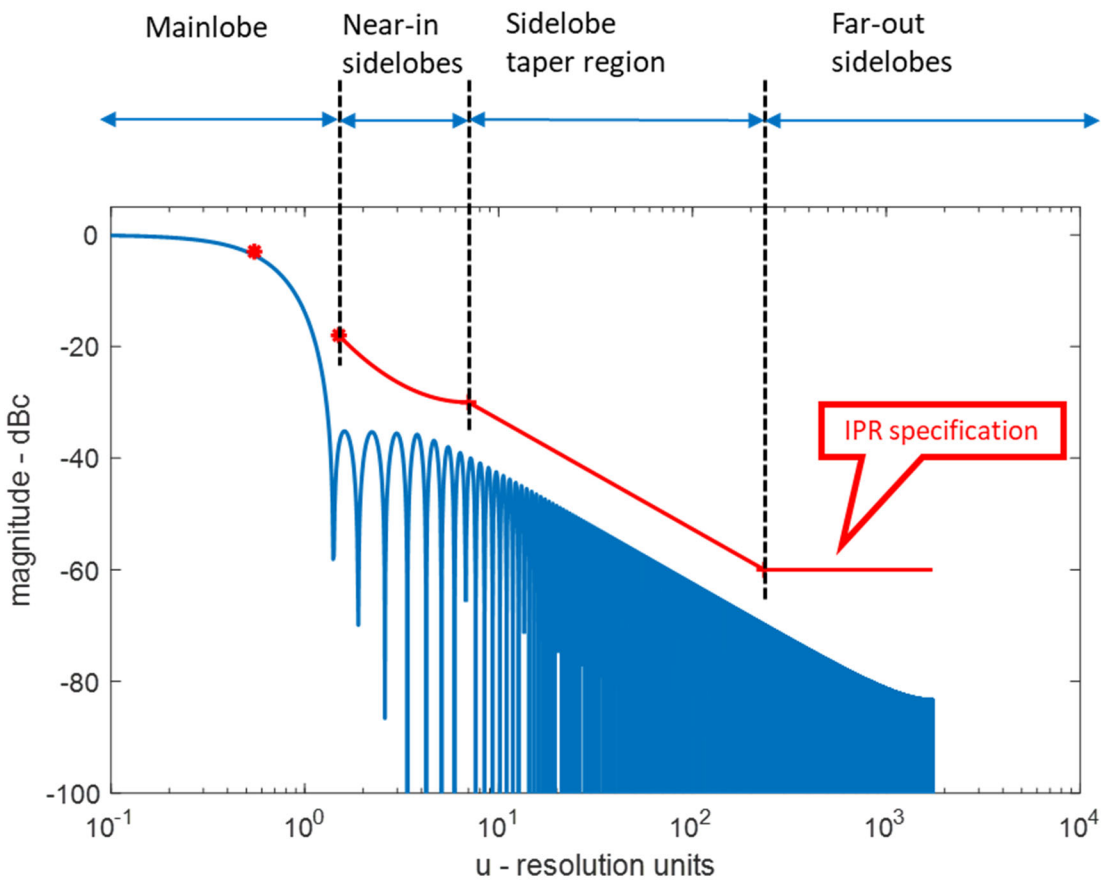

Figure 6. Ideal -35 dB Taylor window taper function with notional sidelobe limit specification and major sidelobe regions identified. Only positive offsets from mainlobe peak are plotted.

Note that the parameter u is in terms of resolution units. That is, the half-power points of the perfect error-free IPR function occur at $u = \pm 0.5$.

The –35 dB Taylor window taper function with these limits are plotted in Figure 6.

While these IPR limits apply to mainlobe width and PSLR levels, it is generally understood that not every sidelobe should be allowed to simultaneously increase to the PSLR limit. Therefore, to preclude this, it may be prudent to also specify an ISLR limit, or similar.

Multiplicative Noise Ratio

With a point target, in the previous sections we concerned ourselves with the localization of the IPR, that is, maximally constraining the localization of echo energy in the SAR image. We considered this good, and signal perturbations and anomalies that prevented this as undesirable. This of course means minimizing the echo energy that manifests in SAR image pixel locations outside of the mainlobe, in the sidelobe regions. Nevertheless, some degree of energy leakage into sidelobe locations away from the mainlobe is inevitable. We may presume that every pixel location in a SAR image will in fact contain some sidelobe energy properly associated with any and all targets located elsewhere in the image.

For any one location in the SAR image, the energy in the accumulated sidelobes at that location from all other targets is termed multiplicative noise. This is in addition to the additive noise to be discussed in the next section.

Consider a uniformly dense distribution of point targets in the SAR image scene, all with similar energy statistics. The ratio of the expected energy from a desired target in that location to the multiplicative noise is termed the Multiplicative Noise Ratio (MNR).

The MNR is a measure of how much sidelobe energy from all sources spills into a given pixel. While it includes sidelobes from all other targets within the scene, essentially the IPR ISLR in both dimensions, there is also a subtlety that MNR includes any energy outside of the nominal IPR mainlobe area, even if a distinct sidelobe does not exist. In addition, MNR also typically includes any aliased energy from targets outside of the nominal scene, as in energy leaking in through antenna sidelobes, or from ambiguous ranges. The accumulation of this energy relative to an average signal level is sometimes described in terms of an Ambiguity Ratio (AMBR). Furthermore, some calculations also include signal quantization and saturation noise due to the ADC as multiplicative noise.[***] Specifically, the ratio of quantization noise energy to an average signal level is often termed Quantization Noise Ratio (QNR). Other components and circuits can also generate quantization noise effects. Carrera, et al.,[51] give us the calculation

$$MNR = ISLR + AMBR + QNR. \tag{24}$$

The bottom line is, MNR may include elements not covered by an IPR specification.

Therefore, it is common to include an MNR limit specification for SAR system design. A typical total system specification might be on the order of less than −11 to −15 dBc, although actual performance numbers approaching within a few dB of the ISLR characteristics of the employed window taper functions are quite common for high performance systems, e.g., perhaps −20 to −22 dBc for systems using the −35 dB Taylor window taper function of Figure 2 in both

[***] Strictly speaking, quantization noise adds to the signal being digitized, and doesn't depend on signal level at the ADC. However, RX gain ahead of the ADC is often adjusted to yield a fairly stable signal level at the ADC. Sometime this is by manual gain selection, and sometimes by an Automatic Gain Control (AGC) circuit. Nevertheless, as a result of the gain adjustment, the quantization noise level somewhat tracks the average signal level, giving it the characteristic of multiplicative noise.

dimensions. A poor MNR manifests as a loss in contrast in a SAR image that cannot be improved by increasing TX signal power.

Since the MNR might include elements not necessarily included in IPR specifications, and to facilitate SAR system design, it is common to provide an MNR budget that apportions limits to various sources of SAR image distortions. Although such lists are often incomplete, they are nevertheless still often useful. Table 1 exemplifies a notional MNR budget. Note that as is typical, the largest sources of multiplicative noise are the window taper function ISLR along with effects of residual motion compensation errors.

Comments

We offer some additional comments on IPR quality measures.

- Shore, et al., published a paper describing a process that automates an estimate of IPR quality from actual SAR images.[52]
- While we have discussed herein IPR quality measures for SAR systems, we suggest that other imaging modalities would have other criteria, and/or other limits for even the same criteria. For example, MTI systems will generally require more substantial signal processing sidelobe mitigation, and stricter control or mitigation of antenna sidelobe energy. Essentially, "good enough for SAR" may not at all be good enough for other radar modes.

Table 1. Notional MNR Budget.

MNR Source	*Required (dB)*	*Design (dB)*
Signal Processing (window taper function ISLR)	-24	-24
Modulations - Motion Error Compensation w/ Autofocus	-15	-20
Modulations - RF Nonlinearities	-20	-30
Modulations - Phase Noise	-30	-40
Spurious - DAC	-20	-30
Spurious - Other	-30	-40
Aliasing - Ambiguous Ranges	-30	-40
Aliasing - Ambiguous Doppler	-30	-40
Aliasing - IF/Video Filters	-30	-40
Aliasing - I/Q Balance	-30	-40
Quantization - waveform generation	-30	-35
Quantization - ADC (5 dB per bit)	-40	-50
Quantization - processing	-30	-60
Allocation Sum	-12.0	-17.7
Suggested Requirement	-12	-15

Bonus Discussion – Speckle

The discussion before now has generally been regarding an impulse target, and how well it can be rendered. However, in a SAR image, we will quite often have regions of distributed or area clutter targets such as fields of vegetation, which will exhibit a grainy appearance in the image. This is "speckle."

Speckle is a manifestation of the inability to resolve multiple scatterers within some area defined by the nominal resolution of the SAR image. These unresolved individual scatterers sum constructively and destructively, in a manner such that the Central Limit Theorem comes into play, where the predicted echo strength can only be described statistically by a 2-D complex circularly-symmetric Gaussian distribution in the complex SAR image, with pixel magnitude exhibiting a Rayleigh distribution. Each pixel within the region of a distributed clutter will have an echo strength that is a member of the ensemble of possible values that the statistics allow and describe.

As such, the pixel value is a legitimate echo strength value for the region with specific resolution area that that pixel represents. However, an adjacent pixel will represent a different region or independent resolution area, and manifest a different echo strength. Thereby a distributed clutter field will exhibit pixels with different echo strengths, each a member of the possible ensemble of values. Pixels farther apart than the radar's resolution will be otherwise uncorrelated. Speckle is nevertheless a true target response. This is the source of the graininess in distributed clutter regions of a SAR image.

Speckle is sometimes referred to as "spatial noise" because of its randomness as a function of spatial position in the image. In spite of this, it is a legitimate target response from the locations the pixels represent. All else equal, increasing TX power will not alter the specific speckle patterns in a SAR image, including the speckle statistics for the specific clutter field. For this reason, speckle is sometimes described to be a multiplicative noise.[53,54]

Since speckle is decidedly not a single impulse phenomenon, it's only impact to IPR quality metrics is via distributed clutter providing the impetus for ISLR being a part of the MNR metric. However, in spite of having multiplicative behavior, speckle specifically is not included in any MNR budget. Nevertheless, speckle does have an impact on image quality at least for some applications, and is worthy of being addressed. It plays a different role in overall image quality, but it does play a role.

Fully developed speckle is unmitigated speckle for which pixel magnitude exhibits a Rayleigh distribution. A common technique for mitigating speckle is to in some sense average pixel magnitudes of multiple SAR images of the same target scene, but each image collected in a manner to avoid coherence of its speckle with that of the other images. This will drive the manifestation of speckle towards a constant value for distributed clutter, usually a function of its statistical mean reflectivity value. This is described as "Multilook" processing, also called Multiple Image Integration (MII). Using more "looks" will increasingly reduce residual pixel value fluctuations, and perhaps reveal low-level target scene features, as is illustrated by simulation in Figure 7. This is judged to be a quality improvement.

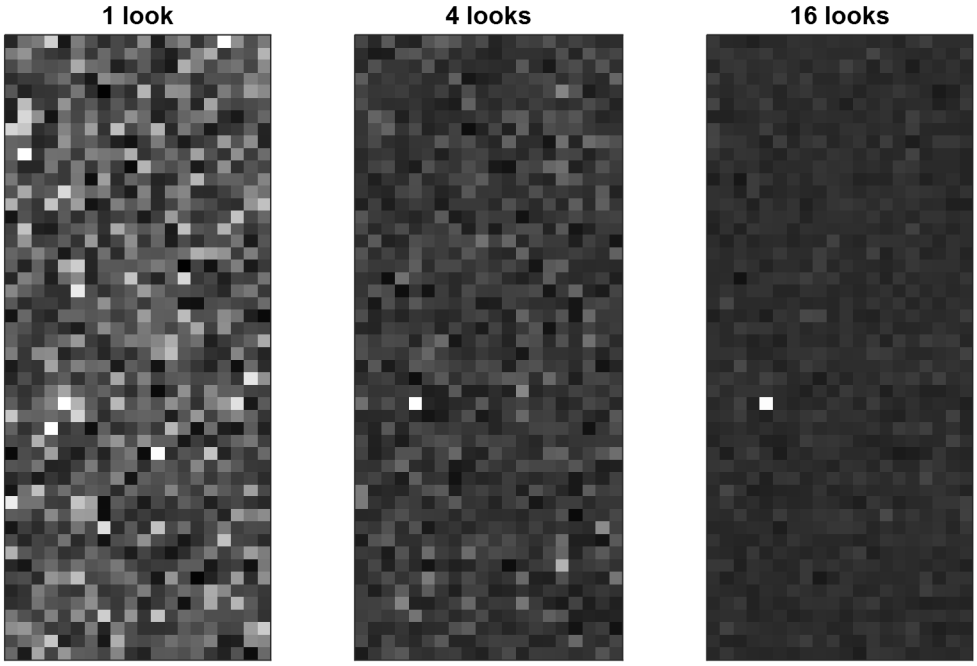

Figure 7. Simulation of speckle with embedded point target response. As more looks are averaged, the point target response becomes more obvious, and the speckled clutter appears more uniform. Images are scaled to provide constant point target magnitude, regardless of number of looks.

Single-image speckle filtering may also be employed. If the image is complex-valued, we might transform to the wavenumber domain and segment the image spectrum, returning the segments separately to the image domain to implement MII speckle reduction.

Alternatively, we might operate on the magnitude image directly, and implement Image Domain Filtering (IDF). Unfortunately, this is also sometimes called "Multilook" processing, but with results significantly different than with MII processing. IDF processing will similarly blur the speckle, but will likewise often coarsen image resolution for point targets, too, although there are sometimes strategies to avoid this to some degree. A wide variety of filtering strategies can be found in the literature. An earlier report compares MII and IDF techniques.[55]

One issue with speckle filtering, regardless of whether MII or IDF techniques are employed, is that pixel phase is usually destroyed. This precludes some further SAR image exploitation techniques, notably those that require coherence between multiple SAR images.

Nevertheless, an implemented or desired amount of speckle reduction is sometimes specified in terms of "equivalent number of looks," or something similar. Other measures can also be found. Gomez, et al., attempt to quantify speckle reduction techniques' effect on image quality.[56]

“If you can not measure it, you can not improve it.”
– Lord Kelvin

3 Additive Noise

We generally consider any undesired energy that competes with our desired echo signal as "noise." In the previous section we dealt with noise of a multiplicative nature, that is, undesired energy that generally tracked the IPR mainlobe in some fashion. Multiplicative noise cannot be overcome by increasing the echo energy, whether by increasing TX power or limiting losses.

We now address additive noise, that is, undesired energy that does not depend on any RX echo signal power. This noise is generally constant regardless of SAR scene content.

As in the previous section, we may parse relevant additive noise sources into related categories.

3.1 Broadband Systemic Noise Sources

Here we offer several different sources of broadband noise. Such noise is generally assumed to be random in nature and uncorrelated from sample to sample, even within a single pulse, and hence considered effectively "white noise." In the SAR image they manifest as a low-level noise floor of complex Additive White Gaussian Noise (AWGN).

A more thorough discussion of much of the following material is given in an earlier report.[57]

Scene Thermal Emissions

Even an ideal SAR receiver must contend with pointing its antenna towards the scene being imaged. By virtue of the target scene having some temperature greater than absolute zero, that scene will emit broadband radiation, including in the traditional radar bands, consistent with Planck's Law.

For typical radar microwave frequencies and below, the 2-sided Power Spectral Density (PSD) of this noise received by the antenna from the target scene emissions is approximately

$$S_{antenna\ noise}(f) \approx \frac{kT_{scene}}{2}, \tag{25}$$

where

$$\begin{aligned} &k = 1.3806485279 \times 10^{-23}\ \text{J/K} = \text{Boltzmann's constant, and} \\ &T_{scene} = \text{scene absolute temperature.} \end{aligned} \tag{26}$$

This formulation assumes perfect radiation efficiency of the antenna as well as perfect emissivity of the target scene.[57] For microwave radar systems, this scene noise emission temperature is generally assumed to be a standard reference temperature, where

$$T_{ref} = 290\ \text{K} = \text{reference temperature.} \tag{27}$$

We acknowledge that the actual noise PSD received from the scene in Eq. (25) will be scene dependent, with different scene temperatures in summertime Sahara desert versus wintertime South Pole, variations in efficiency and emissivity notwithstanding. Nevertheless, using the reference temperature in Eq. (27) is a good 'average' value useful for analysis and design purposes.

Radar System Noise

Alas, real SAR systems are not 'ideal' and will contribute their own internally-generated noise energy to that received by the antenna. This internally-generated noise originates within the components and circuits of the radar hardware. It is customary to model any added noise by a component as an equivalent noise added to the input of the otherwise ideal component. This is also true for RX circuits in general.

The combined system PSD is then

$$S_{system}(f) \approx \frac{kT_{scene}}{2} + \frac{kT_{internal}}{2}, \tag{28}$$

where

$$T_{internal} = \text{internally-generated equivalent noise temperature.} \tag{29}$$

The tacit assumption here is that $T_{internal}$ is also referenced to the antenna port where T_{scene} is referenced. This internally-generated noise may itself be temperature dependent, although often only a nominal average value is used.

Often, the addition of this internally-generated noise to the noise received by the antenna is treated by scaling the reference temperature so that the 'effective' noise at the otherwise ideal radar's input is

$$S_{system}(f) = \frac{1}{2} kT_{ref} F_N, \tag{30}$$

where

$$F_N = \frac{T_{scene} + T_{internal}}{T_{ref}} \approx 1 + \frac{T_{internal}}{T_{ref}} = \text{System Noise Factor.} \tag{31}$$

We distinguish "Noise Factor" from "Noise Figure" by stipulating that "Noise Figure" is the quantity of Eq. (31) expressed in units of dB.

Nevertheless, F_N customarily encompasses any and all broadband noise sources beyond the level described by the reference temperature. As a practical matter, using a constant value for F_N is usually "good enough' for predicting additive background noise levels in SAR images with acceptable accuracy and precision.

ADC Quantization Noise

As previously described, ADC quantization noise is often treated as a multiplicative noise. It is in fact an additive noise in the radar data and constant at the output of the ADC. However, the signal that goes into the ADC is often gain-adjusted in some manner based upon its received magnitude. Sometimes this is via an Automatic Gain Control (AGC) circuit, and sometimes it is a result of a less-automatic gain adjustment based on expected signal levels.[58] The net result is that the quantization noise 'relative to the signal level' of the radar echo is approximately constant, making it behave as somewhat multiplicative in nature. This is especially true for strong signal levels that may require RX gain attenuation that pushes thermal noise (and equivalent) to levels below the quantization levels of the ADC.

Nevertheless, the quantization noise can be included into calculations of the Noise Factor/Figure for the radar receiver data, and ultimately in the SAR image, although the Noise Factor/Figure will be even more so RX gain dependent.[58]

Other Common Broadband Noise Sources

The model for noise received by the antenna given in Eq. (25) presumes that this is due exclusively to thermal emissions of the target scene being imaged. This is a good model for microwave radars, but fails to account for some other factors that become significant at lower frequencies sometimes also used for SAR, especially below 1 GHz. Below 1 GHz, significant contributors to broadband noise include galactic noise, atmospheric noise, and man-made noise.[59]

Galactic noise stems from the sun and other extraterrestrial sources. Atmospheric noise stems mainly from lightning and atmospheric constituents. Man-made noise in this context includes electromagnetic emissions from all manner of electrical and electronic equipment from spark plugs to digital hardware. Each of these tend to vary with frequency, typically diminishing as frequency increases.

From the International Telecommunications Union (ITU),[60] we observe that below about 5 MHz, atmospheric noise can dominate, but is not guaranteed to do so. Above this, man-made noise will generally dominate until it falls below 290 K somewhere near 1 GHz. However, near a city, at 100 MHz it may exhibit a median value of perhaps 20 dB above to 290 K reference value. Contributions of galactic noise will generally be below the other sources, with the exception of looking directly into the sun.

Other Broadband Transmissions

Here we mention with little to no elaboration some additional sources of broadband noise or noise-like signals. These may be potentially found in any radar band across the spectrum.

Other spectral cohabitants of the radar bands can appear as unintentional wideband noise to the radar. This includes communication services, control signals, as well as other radars.

Of course, we must also mention purposeful broadband jammers that are intended to elevate a radar's noise level to render radar echo data unusable to the operator.

Noise Equivalent Reflectivity

The cumulative additive broadband noise discussed above in this section (from all the sources mentioned) will manifest in a SAR image as a low-level noise floor to the image. In a complex SAR image, it will manifest much like distributed clutter, exhibiting a 2-D complex circularly-symmetric Gaussian distribution with the same spatial correlation, i.e., exhibiting speckle with Rayleigh distribution in a magnitude image. In fact, this noise looks so much like distributed clutter that we can describe it in terms of an equivalent distributed clutter level.

Recall that unlike a specular reflector such as a point or impulse target, a distributed clutter field with uniform clutter statistics is characterized in terms of a normalized Radar Cross Section (RCS) per unit area. Accordingly, it is customary to define the clutter reflectivity as

$$\sigma_0 = \text{normalized clutter reflectivity.} \tag{32}$$

This describes the echo characteristics of a distributed clutter field in terms of RCS per unit area of clutter. The expected power in a SAR image pixel will be proportional to this. Tables and plots of clutter reflectivity values are well documented in the literature.[61,62]

We define the average noise power in the SAR image as

$$\sigma_N = \text{average noise level in the SAR image.} \tag{33}$$

A hypothetical clutter reflectivity value for which $\sigma_0 = \sigma_N$ is called the Noise Equivalent Clutter Reflectivity value, and is a common description of noise level in a SAR image. This goes by several names in various literature, including

Sigma-Noise,
Sigma-N,
Noise-Equivalent Reflectivity (NER), and
Noise-Equivalent Sigma Naught (NES0).

Of note is that the noise level is thereby described in the same terms as clutter, namely in units of RCS per unit area, specifically with units m^2/m^2, or more often transmogrified to units $dBsm/m^2$. How these parameters relate to SAR performance overall is described in an earlier report.[63] Increasing noise levels will increasingly mask low-reflectivity areas causing a loss of contrast in the SAR image, as illustrated in Figure 8.

It is also important to note that within a SAR image, even for uniform clutter, the ratio of expected clutter power in a pixel to the noise power in a pixel is not generally constant across the image. It varies with position in the image. This is because the manifestation of clutter will be subject to range loss within the image as well as antenna pattern attenuation across the image, whereas the noise is not. Consequently, where a single σ_N is specified, it is generally meant to describe the SAR scene reference point, often the center of the image.

Figure 8. Ku-band SAR image of US Capitol building with various NER levels.

Since additive noise clearly impacts image quality, it is common to design SAR systems with a maximum NER specification for a required operating geometry, etc. Of course we would normally only consider natural noise sources, or those man-made sources that could be reasonably expected during operation.

For many SAR image exploitation tasks, a common NER specification for X-band and Ku-band is in the neighborhood of –25 dBsm/m^2. Since for many distributed clutter fields σ_0 is approximately proportional to frequency, we might also justify specifying a maximum σ_N that is also proportional to frequency. For example, an L-band system might use a NER specification of perhaps –35 dBsm/m^2.

We also note that exploitation techniques that rely on coherence between multiple SAR images might wish a lower noise level yet, perhaps something approaching 10 dB lower than otherwise.[64]

3.2 Other Additive Anomalies

In the previous section we addressed additive broadband (generally spectrally white) noise sources. Here we discuss a miscellany of additional additive 'noise' sources that may not fit the broadband characteristics of the previous section. These noise sources are often more commonly called "interference" sources.

Spurious Interference

Radar electronics are replete with all kinds of signals. These signals can leak away from their desired signal paths, and unintentionally enter other components and circuits by combinations of conductive paths and radiated paths. Narrow-band signals in particular are often called "spurious" signals. They may manifest as undesired anomalies and artifacts in SAR images. Furthermore, they may appear anywhere in the SAR image, and even move in apparent image location from one SAR image to the next.

One particular spurious signal that seems to be more common than others is a result of LO leakage in quadrature mixers or DC biases in signal paths (especially at the ADC input), and appears at zero range and Doppler offsets (DC point in the SAR image). It goes by the rather unimaginative name of "DC Dot."

Although additive in nature, spurious signals may enter the signal path anywhere in the RX channel, i.e., on either side of any RX gain attenuators. Consequently, as with quantization noise, they may at times seem to behave in a multiplicative fashion.

Hostile Electromagnetic Interference

We have defined SAR image quality as a function of a user's ability to exploit the image product. An adversary might wish to prevent this, by diminishing the useability of the SAR image, or merely the trust in it, and the SAR system generally. There are a multitude of ways for an adversary to do this.[65]

We may divide techniques for reducing SAR image quality into two main categories.

1. Jamming is an overt degradation of the functionality of the radar. The radar is effectively 'blinded.'
2. Spoofing is fooling the radar into falsely thinking that the target scene is providing information that in truth isn't there, i.e., the radar is providing "fake news."

SAR image susceptibility to jamming and spoofing, along with countermeasures, and counter-countermeasures, is a rich area of study and analysis, well beyond the scope of this report. Direct jamming or spoofing the radar echo is inherently additive in nature, although a clever adversary might make it look otherwise.

Nevertheless, a SAR suffering from jamming or spoofing clearly is offering a degraded quality of its product.

Unintentional Interference

While an adversary might wish to intentionally degrade image quality via jamming or spoofing, even non-adversarial emissions might unintentionally provide a hostile electromagnetic environment. Unintentional jamming happens especially when the spectrum is shared between radar and other users such as communication systems, as is increasingly the case. An example of this is shown in Figure 9.

This sort of interference is inherently additive in nature.

Figure 9. SAR image of a collection of vehicles imaged at L/S-band (2.16 GHz center) exhibiting 0.23-m resolution, corrupted by wireless digital service emissions.

Requirements and Mitigation

Measures and limits for these other additive anomalies are inconsistent in the SAR community. Clearly, we desire them to be low to the point of being inconsequential to exploitation techniques we wish to employ.

We desire these interference sources to be As Low As is Reasonably Achievable (ALARA). To first order, we really desire them to be below the clutter level in the SAR image. Better yet would be for them to be below the noise level in the SAR image.

Mitigation strategies for these additive interference sources will generally be highly dependent on the exact nature of the interference. In general terms, we might initiate the following mitigation strategy in order.

1. Avoidance of the problem by good design practices and operational constraints, including optimum waveform selection.
2. Moving the problem away from the SAR image region of interest by signal processing techniques.
3. Smearing the problem energy to diminish its coherence by signal processing techniques, thereby reducing its manifested peak value in the SAR image.
4. Suppression of the problem directly in the image by appropriate filtering, excising, etc.

4 Other Factors

If we stipulate that image quality is a perception of the user, then we must acknowledge that a wide range of other factors will impact the utility of any particular SAR image for some specific exploitation tasks, regardless of how exquisite or stunning the SAR image might be of which the overall system is capable.

4.1 Imaging Geometry

Consider an ideal SAR system operating flawlessly. The limit on 'goodness' of the SAR image that the system creates might in fact be limited by the circumstances of the raw data collection itself, notably the geometry of the data collection.

We now briefly mention several data collection geometry parameters that will impact the nature of SAR data and hence ultimately SAR image quality.

Grazing Angle

SAR determines ground-range from slant-range measurements. The ratio between the two depends on the cosine of the local grazing angle. Therefore, grazing angle has a strong impact on our interpretation of ground position of a scatterer.

Note that for a non-flat target scene, we must remain mindful that tall objects will exhibit layover, as described in Appendix B, but will also mask or shadow scatterers behind them. Shallow grazing angles will reduce layover, but allow longer shadows. Steeper grazing angles will reduce shadows, but allow more severe layover effects. Consequently, selecting a grazing angle with which to collect the raw data requires accommodating a trade-off between shadow length and layover effects.

Another impact of shallow grazing angles is the reduction of the distributed clutter reflectivity as grazing angles become shallower. This is sometimes modelled via the "constant gamma model" for clutter, where clutter reflectivity varies as[66]

$$\sigma_0 = \gamma \sin \psi_g , \tag{34}$$

where

ψ_g = grazing angle, and
γ = clutter gamma (constant for some clutter type). (35)

Anecdotally, this model seems to work reasonably well for grazing angles less than about 60 degrees. An example of a shallow grazing angle SAR image is given in Figure 10.

Also anecdotally, the 'sweet spot' for airborne microwave SAR images seems to be for grazing angles between about 10 degrees and perhaps 45 degrees. Nevertheless, grazing angles outside this range can still provide quite useable SAR images for many applications.

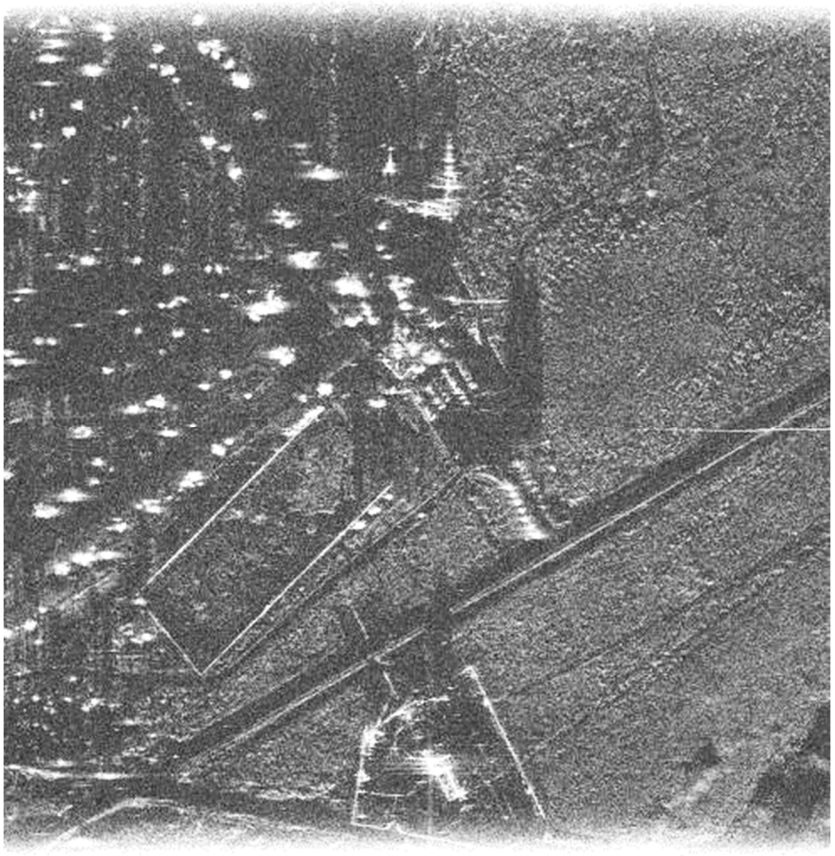

Figure 10. Ku-band SAR image of Kirtland AFB golf course at 0.3-m resolution and 3-deg. grazing angle. Note the long tree shadows that obscure much of the upper left quadrant of the image. The distributed ground clutter is also significantly dimmer than with less shallow grazing angles. Nevertheless, the image is still quite useful for many applications.

Squint Angle

Most SAR systems operate at squint angles fairly near to broadside to the radar's flightpath, seldom squinting more than 45 degrees from broadside. Nevertheless, SAR images can indeed be formed at more severe squint angles, in directions significantly more forward or more aft than 45 degrees from broadside. The cost is ever more layover in the SAR image, noting that the layover is towards the flightpath and not towards the radar itself, as described in Appendix B.

Out-of-Plane Motion

Quite often we simply assume that the SAR exhibits a straight-line flightpath while collecting its data. However, this is perhaps somewhat overly hopeful in many cases. Recall that layover is a function of the flight direction of the SAR, so if the direction changes during the synthetic aperture, especially with out-of-[slant] plane motion, whether intentional or otherwise, then so too does the instantaneous layover characteristics. A changing layover direction represents an unanticipated migration of an elevated target during the collection, and hence a resulting misfocus of the elevated scatterer. Limits on the misfocus due to an elevated offset of a target scatterer from the focused ground-plane is termed the Height-of-Focus for an image.[25]

4.2 Metadata

Now consider an eye-watering perfectly focused low-noise SAR image. However, also consider that it is devoid of basic information of where and when the underlying data was taken. One must then wonder how useful the image then is for time-critical geolocation with respect to a search. With no utility for exploitation, what real quality does it offer?

The collection of useful auxiliary information with respect to a SAR image is often called "metadata." Below we suggest some useful metadata, fully acknowledging that the list is incomplete, and always will be given the plethora of exploitation options available to us. Our intent in this report is to merely illustrate the breadth of potentially useful metadata without any detailed elaboration. Some of these metadata categories might even overlap somewhat.

Geospatial and Temporal Mensuration

Fundamental to many SAR image exploitation tasks is to know where and when the scene was imaged. This might include

- The location of the scene in the SAR image.
- The time the image data was collected.
- The geospatial orientation of the SAR image.

A notion of the accuracy and precision of these parameters might also be useful.

Data Collection Parameters

A number of data collection parameters are important for various exploitation tasks. These might include

- The nominal signal frequency or radar band.
- The data collection geometry, i.e., range, grazing angle, bearing to scene, basic flightpath information, etc.
- Basic antenna parameters, including polarization, etc.
- Any real-time corrections that were applied that would impact the wavenumber domain region of support.

Processing Parameters

Often useful to understand the idiosyncrasies of the SAR image are a number of descriptors of the SAR image. These might include

- Basic IPR characteristics, including description of window taper functions employed.
- An indication of the Image Formation algorithm that was used to form the image.
- Image resolution, especially along principal axes.
- Pixel spacing, or pixel tessellation more generally.

- Pixel characteristics more generally, e.g., complex vs. real-valued, any non-linear scaling applied, etc.
- Any post-processing or other image enhancements that were applied to the image, e.g., autofocus, speckle reduction, etc.

Spatial Fidelity Characteristics

While we have mentioned above the geospatial mensuration of a SAR image, we might dig a little deeper and include

- Parameters that allow geospatial location of all relevant SAR image pixels. This gives us an understanding of the geometric distortions that a SAR image might exhibit.
- Characterization of layover and height of focus.

These topics are inextricably linked to the subject of image projections, and especially a discussion of slant-plane vs. ground-plane images. We tilt at this windmill in Appendix B.[†††]

Image Calibration Parameters

For many SAR image exploitation algorithms, we require reasonably accurate and precise calibration of the radiometric correspondence of SAR image pixel values. We need to know the RCS that a pixel value represents.

Unless corrected or compensated, we must recognize that this relationship might be spatially variant, that is, it is not the same in all parts of the SAR image. As previously mentioned, this might be due to range losses across the image, and the effects of antenna beam patterns. Since these effects are essentially deterministic, the SAR image can be corrected or compensated for them. Consequently, it would then be useful to know whether any compensation was applied, and if so, what the compensation was intended to achieve, e.g., constant proportionality between pixel power and radar reflectivity.

Of course, if any spatially-variant radiometric calibration was applied, then we must acknowledge that the background noise level might be affected so that it now becomes spatially variant. In this case, we might want to know the nature of the spatial dependance of the noise levels.

[†††] Reference: *Don Quixote*, by Miguel de Cervantes, 1605.

4.3 Miscellaneous Comments

We now offer several miscellaneous brief comments.

- The utility of a SAR image and its metadata is considerably enhanced if a user can actually access the information he might be after. Duh.

  The best way to address this is to employ some well-known, and well-documented, standard SAR image format. The SAR image format should allow adequate image representation as well as metadata for the desired exploitation task.

  That is not to say that one-off or proprietary image formats aren't useful, and might even be necessary, but it is likely that some well-designed standard format might be more useful to a wider audience, especially if it allows the addition of user-defined parameter fields to compensate for otherwise missing desired metadata. At the time of this writing, one such SAR image format is the Sensor Independent Complex Data (SICD) format.[67]

- When image compression is applied to SAR images to reduce file sizes, especially lossy image compression, there is always a concern that SAR image quality might suffer excessively. This has been studied and reported by several authors.[68,69,70]

- Heretofore we have discussed image quality in terms of an image represented by data. However, we could have an exquisite high-fidelity SAR image, with an abundance of metadata, in a well-defined and documented file format, and still make it unusable to an analyst by rendering poorly on a display device. So, when a human user is required to examine the image, another aspect of usability, and hence quality, is the display device's capabilities and characterization, and how they match what a human observer requires of the SAR image data. This is discussed in detail in an earlier report.[71]

  LaMonica presents a report that discusses how various image quality factors impact an image analyst's ability to recognize and designate a wide variety of targets.[72]

- Machine-based image analysis also depends on SAR image quality. Novak investigates and reports on the effects of several aspects of image quality on an Automatic Target Recognition (ATR) system's performance.[73]

- Conventional assessments of SAR image quality typically consider only the reflected echo signal from a target of interest, real or theoretical. However, the lack of an echo signal, i.e., the radar shadow, can also impart useful information for exploitation.[74] Assessing the utility of a radar shadow for exploitation will often require additional, different, or even contradictory metrics.[75,76] A discussion of radar shadow quality is beyond the scope of this report.

"When you can measure what you are speaking about, and express it in numbers, you know something about it."
– Lord Kelvin

5 Subjective Image Interpretation Measures

Those charged with tasking SAR image collection missions, as well as those tasked with SAR image analysis and interpretation, are often radar muggles. That is, they don't dwell on objective image quality parameters such as numerical resolutions, noise levels, IPRs, and other engineer-speak. Rather, their intent is to exploit the SAR image to garner information they seek, i.e., what the image is capable of telling them relevant to their operational needs.

To this end, a subjective image interpretability scale has been developed called the National Image Interpretability Rating Scale (NIIRS). This scale rates the interpretability of an image on a scale from 0-9. Higher interpretability numbers imply higher fidelity, allowing characterization of smaller and finer features. Although scales exist for several imaging sensor modalities (e.g., visible, infrared, etc.) we concern ourselves here with the scale developed for SAR imagery. This scale for SAR images is often referred to as Radar-NIIRS, or RNIIRS.

Irvine provides a good short history and methodology used for developing the NIIRS scale.[77] Other papers also discuss history and methodology, and provide useful references, although some of those references can be difficult to procure.[78,79] At this time, a good reference for NIIRS criteria is a standardization document issued by the US National Geospatial-Intelligence Agency (NGA).[80] The collective SAR image NIIRS criteria from this NGA standard are listed in Appendix C.

Of course, especially for tasking, but also to facilitate automated ratings, we need to relate the subjective NIIRS criteria to more objective radar parameters. That is, we desire to predict NIIRS levels from functions of basic radar collection and image parameters. An equation that does this is called a General Image-Quality Equation (GIQE).

While many publications exist discussing GIQE for optical and even infrared sensors, the number of publications regarding development of a good GIQE for SAR systems have been somewhat anemic by comparison, but some do exist. Driggers, et al., propose a two-step conversion that involves converting from a Radar-NIIRS to an Infrared-NIIRS, and then to a probability of discrimination.[81] Gutchess, et al., also present a GIQE for Radar-NIIRS, but note that Automated Target Detection (ATD) performance prediction requires a modification to the GIQE.[82] Schwartzkopf, et al., propose a more direct GIQE and provide results based on SAR images from the Capella orbital SAR.[83]

Without intending to denigrate efforts to date to develop a good GIQE for Radar-NIIRS, we opine that further research and development in this area might still be useful.

“One accurate measurement is worth a thousand expert opinions.”
– Grace Hopper

6 Comments and Conclusions

Some observations are worth repeating here.

- Quality is a perception of the beholder. If it excels at providing the SAR image analyst what he wants to know, then it is of high quality. If it is useless, then it does not provide the quality he needs.
- SAR images are a rendering of a 3-D world in a 2-D image, with limits on the fidelity with which the scene content can be rendered, and hence the quality of the SAR image. Characteristics of the fidelity of such a rendering can be divided into two main aspects: 1) the IPR characteristics, and 2) additive noise.
- Since quality implies utility for exploitation, other factors also are relevant. These include data collection geometry, and metadata that accompanies the SAR image, as well as other useability features.
- Subjective measures of SAR image quality are also employed, especially by the radar tasking and exploitation communities. A principal subjective quality description is the Radar-NIIRS metric. Equating this to objective radar parameters is accomplished with a GIQE function.
- The ability to create a high-quality SAR image requires such a capability to be built into the radar hardware and software. In addition, it requires proper selection of imaging geometry. Achieving quality is not generally an accident, but rather is a result of foresight in the possible sets of mission requirements.
- Testing can verify quality, but cannot create it.

"It's not what you look at that matters, it's what you see."
– Henry David Thoreau

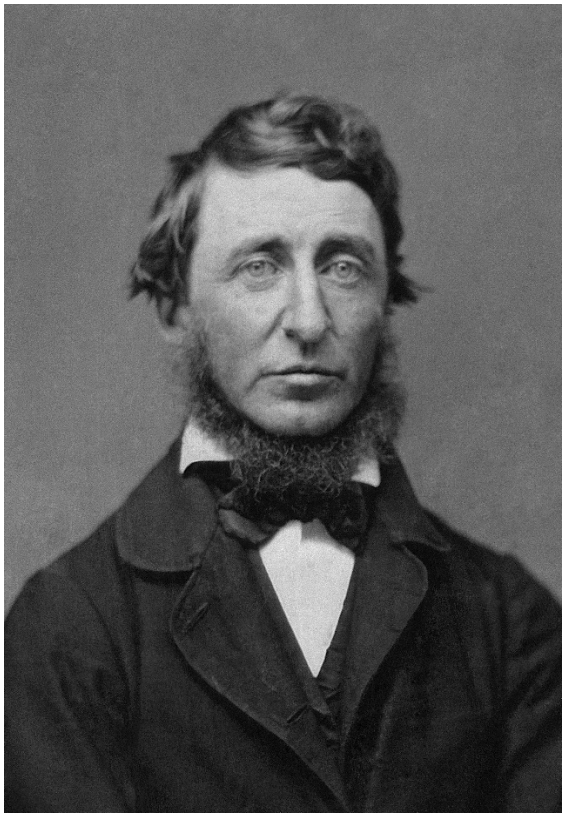

Figure 11. B. D. Maxham daguerreotype of Henry David Thoreau, aged 39, made in 1856. (image courtesy of National Portrait Gallery)

Appendix A – Resolution, What is it?

One of the key parameters in image quality and radar performance assessment is resolution. From Webster's resolution has a couple related definitions:

a) The process or capability of making distinguishable the individual parts of an object, closely adjacent optical (*par* radar) images, or sources of light (*par* radar reflections)
b) A measure of the sharpness of an image or of the fineness with which a device (*par* radar) can produce or record an image …

In imaging systems, such as imaging radars, resolution is a unit measure that relates the proximate closeness that permits two independent pieces of information to be distinguished. Typically, and for our purposes, radar resolution refers to spatial resolution or closeness in distance within radar images. More generally, resolution could also refer to other radar measurements, such as target velocity measurement, target power measure, etc.

The concept of resolution is actually complicated to define. There are different definitions of resolution that have arisen in the imaging community through the years due to attempts to simplify and standardize the concepts that are behind the fundamental ability to distinguish close objects within an image. How do we best determine a measure of this separation? A good discussion of the different definitions for resolution is given by den Dekker and van den Bos.[84]

Historically resolution definitions for imaging systems come from work in the optics community. Although there are some differences with respect to the nature of resolution between optics and radar, they are strongly related. So much so that much of the resolution concepts and definitions in radar have evolved from optics.

The most common definition of resolution in radar system design and image quality evaluation is an evolution of that originally proposed for spectroscopy by John William Strutt, better known as Lord Rayleigh.[84,85] Lord Rayleigh's original definition was:

> *"… an angular interval that the central line in the image of one coincides with the first zero of brightness in the image of the other."*[85]

In terms of SAR images, the "central line" is the center of the Impulse Response (IPR), in other words the location of peak of the response to an idealized point target. The "first zero" is the first null from the peak response.

The original Rayleigh definition of resolution has been adapted in radar literature to be the distance between the half-power points of the IPR, or analogously the Point-Spread Function (PSF) in optics. This more closely resembles the definition of resolution proposed by Houston.[86] It is common to simplify this as the distance between points on opposite sides of the peak of the IPR that are 3 dB down from the peak response since $10\log_{10}(0.5) \approx -3.0103$.[11] Figure 12 shows the idealized impulse response to a point target for two different processing window taper functions.

Figure 12 shows us ideal analytical impulse response functions. This leads us to an important distinction between two related concepts. The first is an analytical or predicted value of the IPR. This often relates to Key Performance Parameters (KPP) in comparing proposals for new systems. The second is an actual measured value of the half-power resolution of a system's impulse response function. This is the concept that relates to image quality. Ideally, these two values should be relatively close in value.

As mentioned in the main body of this report, the conventional monostatic SAR images are 2-dimensional images. The radar measures dimensions that are range, and range rate (due to cross-range offset) that are filtered into a specific k-space wavenumber region of support (Section 2.1). The resolutions in the two directions are a function of the bandwidths in each direction of the region of support. Note that support region is in 3-D space that is most commonly projected into 2-D space by projecting onto $k_z = 0$. This corresponds to a specific constant ground height, i.e., the presumption of a flat target scene. Generally, SAR does not resolve in the spatial frequency dimension orthogonal to the 2-D k-space, leading to the concept of layover.

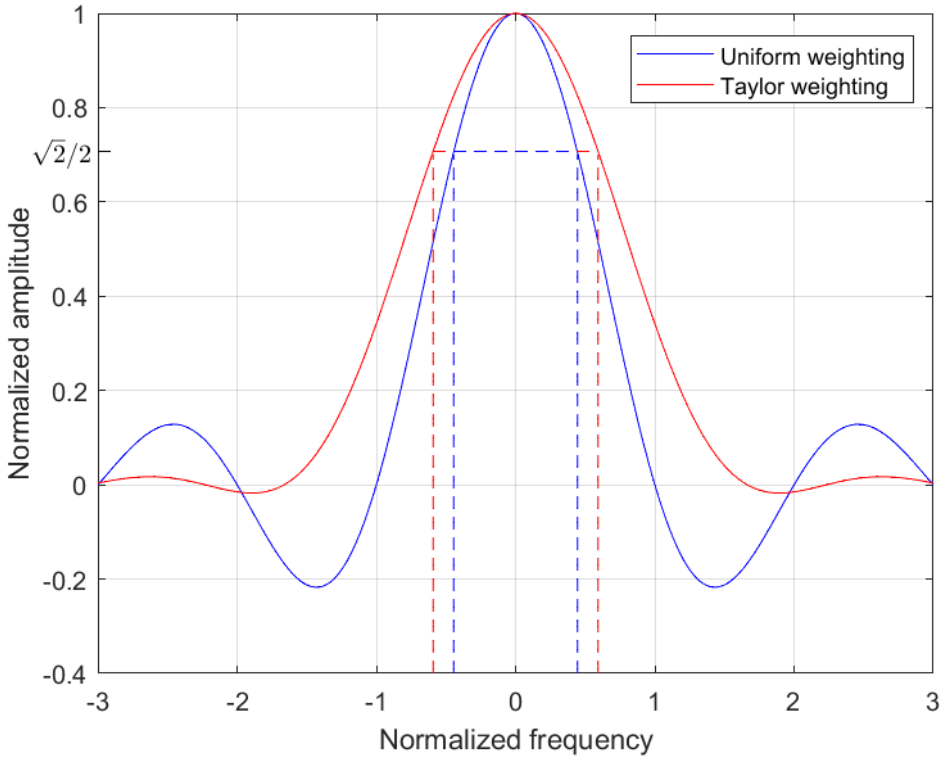

Figure 12. Example of resolution for uniform weighting and Taylor weighted impulse response functions

The analytical equation for Rayleigh (slant) range resolution provided large time-bandwidth product is given in various references as [41,87]

$$\rho_r \approx \frac{a_{wr} c}{2 B_r} \tag{A1}$$

where

a_{wr} = the IPR spread factor due to signal processing in the slant-range dimension (e.g., processing window tapering),
c = the speed of light, and
B_r = the received bandwidth of the processed pulse. (A2)

It is common to project this resolution from the slant range to the ground (y-direction) in which case the resolution in the equation is scaled by the reciprocal of the cosine of the local grazing angle.

The cross-range dimension resolution is given by [41,87]

$$\rho_x \approx \frac{a_{wx} c}{2 f_c \Delta\theta} \tag{A3}$$

where

a_{wx} = the IPR spread factor due to signal processing in the azimuth dimension,
f_c = the center frequency of the received pulse, and
$\Delta\theta$ = angular extent of the support of the k-space aperture. (A4)

Note that $f_c \Delta\theta$ is effectively a bandwidth in the cross-range dimension.

The above is by far the most common definition of resolution for monostatic SAR systems, however even Rayleigh acknowledges limitations on his definition

> "*This rule is convenient on account of its simplicity and it is sufficiently accurate in view of the necessary uncertainty as to what exactly is meant by resolution.*" [85]

Other definitions for resolution have been developed through the years and are used in an effort to better quantify information available in radar images. This is particularly true as signal processing techniques are used that attempt to improve on Rayleigh resolution.[84] Many of these resolution definitions were developed with a purpose to account for noise and unpredictable systematic errors that require statistical description. A few other resolution definitions are now discussed to provide a flavor of other considerations.

As with the Rayleigh resolution definition, almost all of the resolution definitions assume identifying two separate point targets. It can be observed that under this assumption, resolution can be defined as a measure of closeness that leads to detecting two distinct point sources. For

example, Sparrow's definition defines resolution as the separation between two point sources that just leads to a dip between the superposition of the peaks responses.[88] This definition is extended to cases of other image processing techniques for improved resolution, such as the Capon method also known as the minimum variance distortionless response (MVDR).[89,90] These imaging methods rely on image statistics, in particular estimation of the covariance matrix. The corresponding resolution measure is also developed from a statistical viewpoint as a "probability of detection" which is the probability of observing the dip in the presence of interference from noise, clutter, jamming, etc.[90,91] Necessarily, probability of resolution extends the definition of resolution to take into account signal-to-interference-plus-noise ratio.

More recently definitions of resolution are further extended using information theory which also accounts for signal-to-noise ratio as well as bandwidth (see references on this subject in den Dekker and van den Bos[84]). An important case of the use of information theory in generalized resolution is the development of equations to assess image quality, such as Radar Generalized Image Quality Equation, aimed at predicting human interpretation of radar imagery.[83]

There are other resolution considerations outside the scope of this document, such as resolution in low-frequency non-rectangular k-space apertures.[92] Bistatic SAR system resolution equations and definitions are discussed in a report by Doerry,[93] and a paper by Vu.[94]

Work in studies of radar resolution will continue. The basis is that we want to specify the density of information available in radar imagery. Although it continues, currently the measured Rayleigh resolution for a point target in a low noise/clutter background remains the classical measure for image quality assessment.

Appendix B – Slant-Plane vs. Ground-Plane SAR Images

There is much mythology and misconception around a too-frequently asked question about some SAR image, that being "Is this a slant-plane image or a ground-plane image?" We now examine these descriptions and what they really mean, and how they compare.

Background

We begin by noting that a single SAR image is indisputably a 2-D projection of a 3-D scene. That is, there is some degree of 'collapse' of a third dimension of the 3-D world. Inherent to SAR is that the imaging process distinguishes pixels by unique combinations of range and range-rate. For a SAR instrument collecting data along a straight-line level flightpath, for any point along the flightpath a constant range defines a sphere, and a constant range-rate defines a cone with central axis coinciding with the flightpath. Their intersection is a circle that is in a plane normal to the flightpath. This is illustrated in Figure 13. We define the ground plane as a locally horizontal plane at the SAR image Scene Reference Point (SRP).

This circle intersects the ground plane at as many as two places, one on either side of the flightpath. Of course, the antenna illuminates only one of these, expecting a pixel in the SAR image to represent echo energy from just this one location, having assumed a flat target scene. However, any other target echo from anywhere else on this circle will exhibit the same range and range-rate, and therefore manifest any echo energy in the same SAR image pixel, i.e., project or lay over onto the same image pixel location.

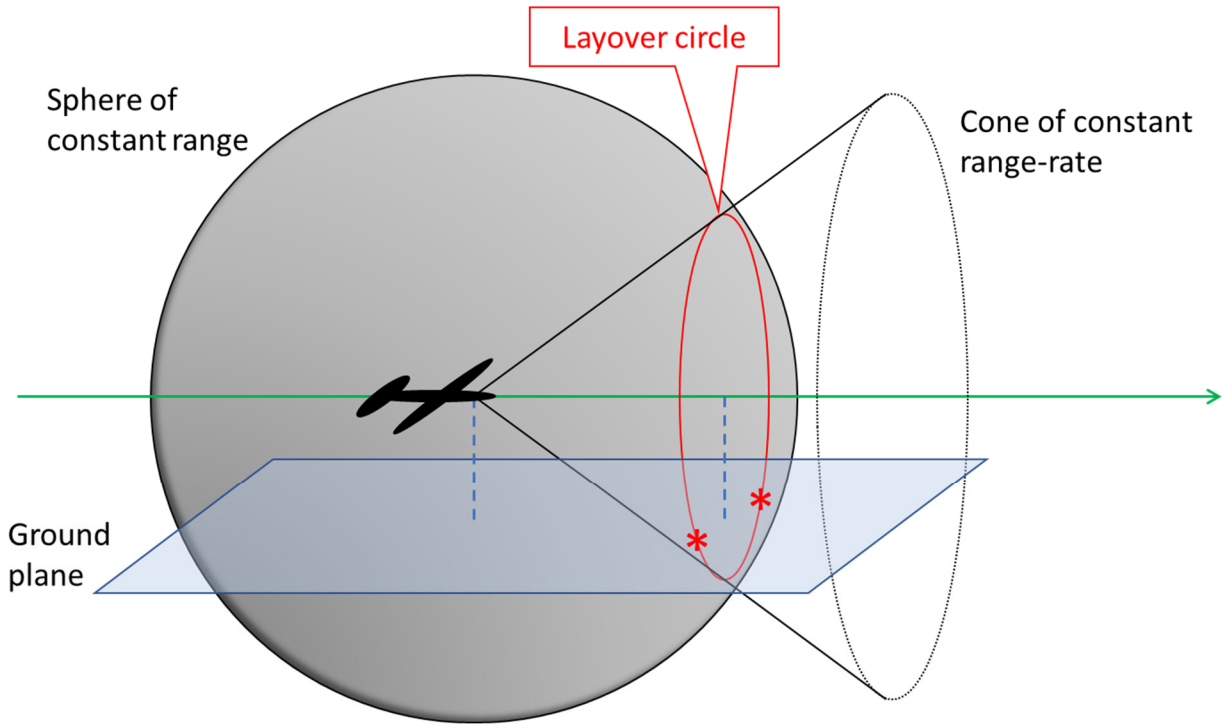

Figure 13. Geometry of constant range and range-rate for SAR data collection.

Of great significance is that this layover circle is fundamentally due to the flightpath itself, and not dependent in any way on the image formation algorithm employed to form the SAR image. This layover circle defines the arc of projection. It is baked into the raw data itself.

Furthermore, in the absence of any additional information, the SAR generally inherently assumes that target locations of interest are on the ground plane, so the image is focused to the ground plane, again regardless of the image formation algorithm employed to form the SAR image.

[Conventional] Slant Plane

Somewhat colloquially to the SAR community, the "Slant Plane" customarily refers to the plane defined by the radar's straight-line flight path and the SRP. This is illustrated in Figure 14. With malice aforethought, we will refer to this specific slant plane as the "Conventional Slant Plane." Clearly, for an airborne SAR, the conventional slant plane does not coincide with the ground plane. Nevertheless, there is a one-for-one correspondence between locations on the conventional slant plane and locations on the ground plane. The correspondence or mapping is defined by the layover circle discussed above. Note that the specific circle is range-dependent. Circles at different ranges will have different curvatures.

A crucial observation to this discussion is that an arbitrary rectangular grid on the ground plane will not map to a rectangular grid in the slant plane, and vice versa. They will be warped versions of each other.

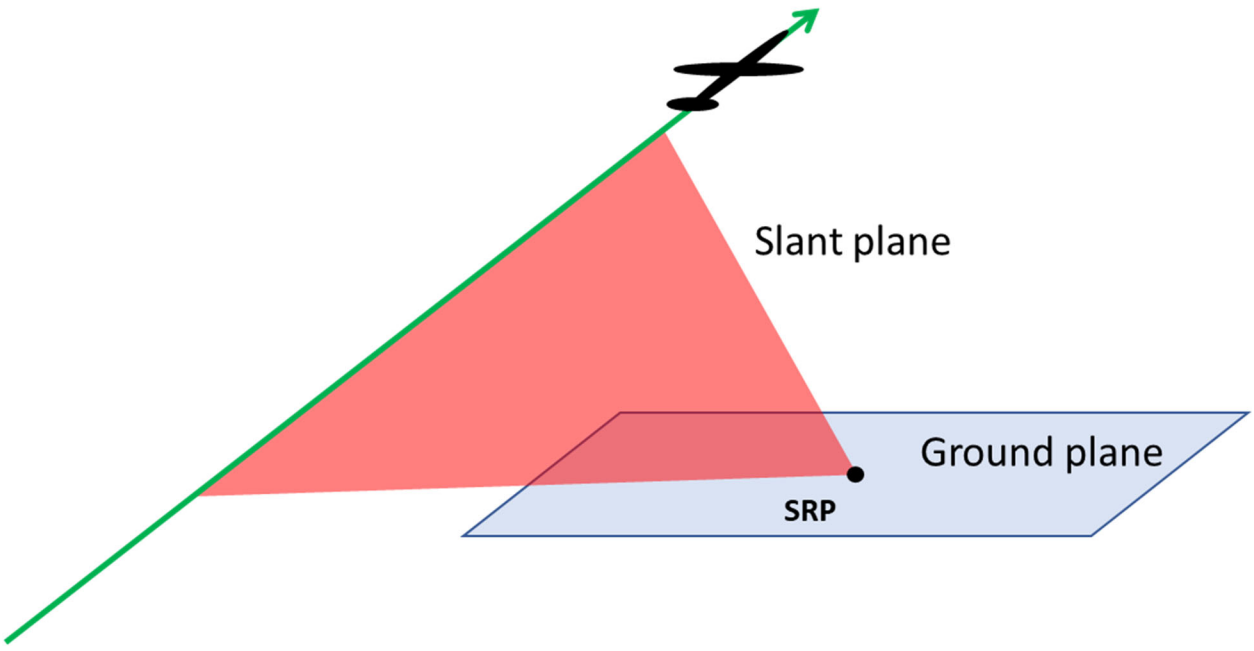

Figure 14. Conventional Slant Plane definition.

Slant-Plane vs. Ground-Plane SAR Images

There is some ambiguity in the literature about what exactly constitutes a slant-plane image vs. a ground-plane image. However, a common distinction is given by the specification for the SICD SAR image data format.[67] They give distinctions that are essentially as follows.

> ***Slant-Plane Image*** – typically defined as one where range pixel increments are constant in slant range, and often cross-range pixel increments are constant in range-rate. These images are said to be projected into what we have termed the conventional slant plane.
>
> ***Ground-Plane Image*** – typically defined as one where range pixel increments are constant in ground range, and typically cross-range pixel increments are also constant in cross-range distance. These images are said to be projected into the ground plane.

We take from these definitions that [conventional] slant-plane images and ground-plane images are merely warped versions of each other. Both are focused to the ground plane that contains the target scene being imaged. Either can be created from the same raw data, with some image formation algorithms favoring one and some the other. Nevertheless, either can also be created from the other. Both contain the exact same information. Neither is 'better' than the other, with perhaps the single distinction that ground-plane images might be easier to match to other planform maps.

Gratuitous Comments

While we have defined ground-plane images, and [conventional] slant-plane images as merely different pixelations of each other, we assert that other pixelations might also be developed and render perfectly good SAR images with no loss of information. In fact, image formation algorithms can be developed that provide renderings with pixel spacings constant in other slant planes. There are an infinite number of such 'other' slant planes.‡‡‡

Conclusions

Some concluding comments include the following.

- Slant-plane images and ground-plane images contain the exact same information.
- Each can be warped to become the other.
- There are in fact an infinite number of slant planes (or other surfaces) to which pixels can be formed or warped.
- Assertions and arguments that a ground-plane or any of the slant-plane images is better than the other often become very annoying very quickly.

‡‡‡ We assert anecdotally without elaboration that as we write this, operational SAR systems are flying every day that form perfectly useful high-quality SAR images that are rendered with pixelations that are constant spacing in other slant planes.

"It all depends on how we look at things, and not how they are in themselves."
– Carl Jung

Appendix C – Radar-NIIRS Definitions

What follows are criteria for Synthetic Aperture Radar NIIRS rating levels, taken from the NGA standard.[80] The criteria are combined from tables for six Orders of Battle: air, cultural, ground, naval, missile, and electronic. Not all orders of battle have criteria for all NIIRS levels.

NIIRS Level 0

Interpretability of the imagery is precluded by obscuration, degradation, or low resolution.

NIIRS Level 1

Determine azimuth of main runway at a large airfield.

Detect lines of transportation, either road or rail, but do not distinguish between.

Detect a large vessel in open water.

NIIRS Level 2

Detect parallel taxiways.

Distinguish between forested areas and agricultural fields.

Detect very large defensive berm.

Detect known ICBM facility.

Detect large freighters or tankers at a known civilian port facility.

NIIRS Level 3

Identify the basic functional areas of an airfield or air base (e.g., hangars, weapons or POL storage, passenger terminals).

Detect multiple wings of large buildings.

Identify a barracks area based on pattern of buildings.

Detect known KRUG site.

Detect Rail Transfer Point (RTP) at missile facility.

Distinguish between ships and floating dry docks.

NIIRS Level 4

Detect large fighter aircraft (e.g., Su-34 FULLBACK, F-15, Chengdu J-20).

Identify wing configuration (e.g., straight, swept, delta) or large aircraft (e.g., BEAR, B1).

Detect smokestacks in industrial facilities.

Detect large vertical lattice mast antenna.

Detect a convoy or preparations for deployment at a motor pool.

Detect coastal defense artillery battery based on location and dispersal pattern.

Identify square bow shape of ROPUCHA LST or GREN LST.

Detect SS/SSN at known port facility (e.g., KILO, TYPE 209, SONG SS, VICTOR III).

Distinguish between DON-class AS and SMOLNYY-class AX ship based on superstructure configuration.

NIIRS Level 5

Distinguish between large bomber and cargo aircraft (e.g., BEAR v. CANDID or B-52 v. C-17).

Detect small helicopters (e.g., HOPLITE, MD 500/530, ALOUETTE).

Distinguish between a large vertical mast antenna and a large power-transmission tower.

Detect a battery of towed artillery (not revetted) based on deployment pattern.

Detect a deployed LOW JACK radar on a vehicular transporter based on position.

Distinguish between SS/SSN and SSBN.

Distinguish between DAXIN-class AXT and DARONG-class AP ship based on superstructure configuration.

NIIRS Level 6

Identify large helicopters by type (e.g., HALO, CHINOOK, SUPER FRELON, SUPER STALLION).

Identify wing configuration of small fighter aircraft as swept, delta, or straight (e.g., MIRAGE 2000, F-16, FROGFOOT).

Detect cargo on a railroad flatcar.

Detect deployed mast-mounted TWIN EAR B/C antenna.

Identify a single vehicle as a large truck (e.g., KRAZ-6300, URAL-63095).

Distinguish between wheeled and tracked vehicles in garrison based on vehicle size and dimension.

Detect a warhead van at a known Rail Transfer Point (RTP).

Identify SS by class (e.g., KILO, TYPE 209, SONG SS).

Identify bow gun on a destroyer.

Detect deployed mast-mounted TWIN EAR B/C antenna.

NIIRS Level 7

Identify medium helicopters by type (e.g., HIP, HIND, SUPER PUMA).

Identify fighter aircraft by type (e.g., FULCRUM, TYPHOON, F-15, MIRAGE).

Detect the break between cab and trailer on a tractor-trailer truck.

Distinguish between electronic van trailers (without tractor) and van trucks in garrison.

Distinguish between THIN SKIN A (trailer-mounted) and THIN SKIN B (truck-mounted) radars.

Determine general function of engineering equipment when in garrison (e.g., bridge sections, boats, earthmovers, and mine laying/clearing).

Distinguish between a turreted, tracked APC and a medium tank by size and configuration (e.g., 9P162 KORNET-E vs. T-90).

Distinguish between Type-3 NOOR TEL and Type-3 NOOR TELAR when in garrison.

Determine if an SA-3 missile launcher is loaded or empty.

Distinguish between OSAI and OSAII PCFGs based on missile canister shape.

Identify closed missile hatches on a DELTA IV SSBN.

NIIRS Level 8

Identify small helicopters (e.g., HOPLITE, MD 500/530, ALOUETTE).

Detect individual rail ties.

Detect the vertical ribs on the antenna of a HIT MAN radar.

Distinguish between PMP center sections and ramp sections when mounted on KRAZ 255 truck.

Distinguish between 2S6 and ZSU23/4 SPAA guns by overall configuration.

Distinguish between CSSC2 SILKWORM and CSSC3 SEERSUCKER missiles.

Determine the location of the running light on the stern fin of DELTA III or ARIHANT SSBN.

Identify the individual RBU tubes on surface combatants (e.g., KIROV CGN, KRIVAK FFG, GRIGOROVICH FFG).

NIIRS Level 9

Distinguish between blade antenna configurations on aircraft models (e.g., IL-76T CANDID vs. IL-76 TD CANDID, HIP vs. HIP C).

Distinguish between models of fighter aircraft (e.g., FLANKER B-C, F-15 A-E).

Identify feedhorn on THIN SKIN B radar when not operational.

Detect both gun tubes on 2S6 SP AAA gun.

Detect exhaust nozzle on solid-fuel booster packs on SA-5 missile.

Detect gun barrels on PHALANX CIWS.

Detect exhaust nozzle on solid-fuel booster packs on SA-5 missile.

References

[1] A. W. Doerry, Vivian Dee Gutierrez, Lars Wells, "A portfolio of fine resolution SAR images," SPIE 2004 Defense & Security Symposium, *Radar Sensor Technology IX*, Vol. 5410A, Orlando FL, 12-16 April 2004.

[2] A. W. Doerry, Vivian Dee Gutierrez, Lars Wells, "A portfolio of fine resolution SAR images - continued," SPIE 2004 Defense & Security Symposium, *Radar Sensor Technology IX*, Vol. 5410A, Orlando FL, 12-16 April 2004.

[3] A. Doerry, D. Dubbert, M. Thompson, V. Dee Gutierrez, "A portfolio of fine resolution Ka-band SAR images: part I," SPIE 2005 Defense & Security Symposium, *Radar Sensor Technology X*, Vol. 5788, Orlando FL, 28 March - 1 April 2005.

[4] A. Doerry, D. Dubbert, M. Thompson, V. Dee Gutierrez, "A portfolio of fine resolution Ka-band SAR images: part II," SPIE 2005 Defense & Security Symposium, *Radar Sensor Technology X*, Vol. 5788, Orlando FL, 28 March - 1 April 2005.

[5] A. D. Sweet , D. F. Dubbert , A. W. Doerry , G. R. Sloan , V. Dee Gutierrez , "A portfolio of fine resolution Ku-band miniSAR images: part I," SPIE 2006 Defense & Security Symposium, *Radar Sensor Technology X*, Vol. 6210, Orlando FL, 17-21 April 2006.

[6] A. D. Sweet , D. F. Dubbert , A. W. Doerry , G. R. Sloan , V. Dee Gutierrez , "A portfolio of fine resolution Ku-band miniSAR images: part II," SPIE 2006 Defense & Security Symposium, *Radar Sensor Technology X*, Vol. 6210, Orlando FL, 17-21 April 2006.

[7] Mark S. Clinard, "Image quality specification and maintenance for airborne SAR," SPIE Defense & Security Symposium, *Radar Sensor Technology VIII and Passive Millimeter-Wave Imaging Technology VII*, Volume 5410, Orlando, Florida, USA, 12 August 2004.

[8] Mark Clinard, Kristo Miettinen, Paul Zavattero, "Spotlight Synthetic Aperture Radar (SAR) Requirements Evaluation Using Phenomenology-Based Image Quality Metrics," Proceedings of SPIE, *Radar Sensor Technology VI*, Vol. 4374, pp. 34-39, 22 August 2001.

[9] R. H. Mitchel, Stanley Marder, "Synthetic aperture radar (SAR) image quality considerations," Proceedings of SPIE, *Image Quality*, Vol. 310, pp. 58-69, 28 December 1981.

[10] R. H. Mitchel, Stanley Marder, "Synthetic aperture radar (SAR) image quality considerations," *Optical Engineering*, Vol. 21, No. 1, pp. 48-55, February1982.

[11] Antonio Martinez, Jean L. Marchand, "SAR image quality assessment," *Revista de Teledeteccion*, No. 2, pp.12-18, November 1993.

[12] Xin Lu, Hong Sun, "Parameter Assessment for SAR Image Quality Evaluation System," *Proceedings of the IEEE 1st Asian and Pacific Conference on Synthetic Aperture Radar*, pp. 58-60, 5 November 2007.

[13] Michele Vespe, Harm Greidanus, "SAR Image Quality Assessment and Indicators for Vessel and Oil Spill Detection," *IEEE Transactions on Geoscience and Remote Sensing*, Vol. 50, No. 11, pp. 4726-4734, November 2012.

[14] R. H. Mitchel, D. A. Ausherman, H. W. Doss, M. 8. Evans, B. H. Friberg, W. D. Hall, *SAR Image Quality Analysis Model – Volume 2*, Air Force Avionics Laboratory Report AFAL-TR-74-114, Unclassified, May 1974.

[15] Armin W. Doerry, *Reflectors for SAR Performance Testing – second edition*, Sandia National Laboratories Report SAND2014-0882, Unlimited Release, Supersedes SAND2008-0396, February 2014.

[16] Mark A. Richards, *Fundamentals of Radar Signal Processing*, ISBN: 0-07-144474-2, McGraw-Hill, Inc., 2005.

[17] Armin W. Doerry, *Anatomy of a SAR Impulse Response*, Sandia National Laboratories Report SAND2007-5042, Unlimited Release, August 2007.

[18] Armin W. Doerry, *Catalog of Window Taper Functions for Sidelobe Control*, Sandia National Laboratories Report SAND2017-4042, Unlimited Release, April 2017.

[19] Armin Doerry, "Bandwidth requirements for fine resolution squinted SAR," *Proceedings of the SPIE 2000 International Symposium on Aerospace/Defense Sensing, Simulation, and Controls, Radar Sensor Technology V*, Vol. 4033, Orlando FL, 27 April 2000.

[20] John Summerfield, Leif Harcke, Brandon Conder, Eric Steinbach, "Bistatic SAR Flight Demonstration using Agile Frequency Waveforms to Achieve Orthogonal Sidelobe Axes," *Proceedings of the 2024 IEEE Radar Conference (RadarConf24)*, pp. 1-6, Denver, CO, USA, 6-10 May 2024.

[21] Armin W. Doerry, Edward E. Bishop, John A. Miller, *Basics of Backprojection Algorithm for Processing Synthetic Aperture Radar Images*, Sandia National Laboratories Report SAND2016-1682, Unlimited Release, February 2016.

[22] Armin W. Doerry, *Basics of Polar-Format Algorithm for Processing Synthetic Aperture Radar Images*, Sandia National Laboratories Report SAND2012-3369, Unlimited Release, May 2012.

[23] Fred M. Dickey, Louis A. Romero, Armin W. Doerry, *SAR Window Functions: A Review and Analysis of the Notched Spectrum Problem*, Sandia National Laboratories Report SAND2002-2949, Unlimited Release, September 2002.

[24] Cameron H. Musgrove, *Interference Mitigation Effects on Synthetic Aperture Radar Coherent Data Products*, Ph.D. Dissertation, Oklahoma State University, 2015.

[25] Armin W Doerry, Douglas L Bickel, *Synthetic Aperture Radar Height of Focus*, Sandia National Laboratories Report SAND2021-0144, Unlimited Release, January 2021.

[26] H.C. Stankwitz, R.J. Dallaire, J.R. Fienup, "Spatially variant apodization for sidelobe control in SAR imagery," *Proceedings of 1994 IEEE National Radar Conference*, pp. 132-137, Atlanta, GA, USA, 29-31 March 1994.

[27] H. C. Stankwitz, R. J. Dallaire, J. R. Fienup, "Nonlinear Apodization for Sidelobe Control in SAR Imagery," *IEEE Transactions on Aerospace and Electronic Systems*, Vol. 31, No. 1, pp. 267-279, Jan. 1995.

[28] F. M. Dickey, L. A. Romero, J. M. DeLaurentis, A. W. Doerry, "Superresolution, Degrees of Freedom and Synthetic Aperture Radar," *IEE Proc.-Radar Sonar Navig.*, Vol. 150, No. 6, pp 419-429, December 2003.

[29] Armin W. Doerry, *Component and Circuit Performance Measurements for Coherent Radar – A Systems Perspective*, Sandia National Laboratories Report SAND2020-5228, Unlimited Release, May 2020.

[30] Armin W. Doerry, Dale F. Dubbert, Bert L. Tise, *Effects of Analog-to-Digital Converter Nonlinearities on Radar Range-Doppler Maps*, Sandia National Laboratories Report SAND2014-15909, Unlimited Release, July 2014.

[31] Armin W. Doerry, *Mitigating I/Q Imbalance in Range-Doppler Images*, Sandia National Laboratories Report SAND2014-2252, Unlimited Release, March 2014.

[32] R. E. Ziemer, W. H. Tranter, *Principles of Communications – Systems, Modulation, and Noise*, Fourth Edition, ISBN 0-471-12496-6, John Wiley & Sons, Inc., 1995.

[33] Tri T Ha, *Solid-State Microwave Amplifier Design*, ISBN 0-471-08971-0, John Wiley & Sons, Inc., 1981.

[34] Armin W. Doerry, Douglas L. Bickel, *Notes on Linear FM Chirp for Radar*, Sandia National Laboratories Report SAND2024-04658, Unlimited Release, April 2024.

[35] Armin W. Doerry, *Transmitter Passband Requirements for Imaging Radar*, Sandia National Laboratories Report SAND2012-10688, Unlimited Release, December 2012.

[36] Armin W Doerry, *Digital Signal Processing of Radar Pulse Echoes*, Sandia National Laboratories Report SAND2020-9428, Unlimited Release, September 2020.

[37] A. W. Doerry, J. M. Andrews, S. M. Buskirk, "Digital synthesis of linear-FM chirp waveforms – comments on performance and enhancements," SPIE 2014 Defense & Security Symposium, *Radar Sensor Technology XVIII*, Vol. 9077, Baltimore MD, 5–9 May 2014.

[38] A. W. Doerry, "An architecture for pre-warping general parametric frequency-modulated radar waveforms," SPIE 2017 Defense & Security Symposium, *Radar Sensor Technology XXI*, Vol. 10188, Anaheim, CA, 9-13 April 2017.

[39] Armin W. Doerry, *Motion Measurement for Synthetic Aperture Radar*, Sandia National Laboratories Report SAND2015-20818, Unlimited Release, January 2015.

[40] Mehrdad Soumekh, *Synthetic Aperture Radar Signal Processing with MATLAB Algorithms*, ISBN: 0-471-29706-2, Wiley-Interscience, John Wiley & Sons, Inc., 1999.

[41] Charles V. Jakowatz Jr., Daniel E. Wahl, Paul H. Eichel, Dennis C. Ghiglia, Paul A. Thompson, *Spotlight-Mode Synthetic Aperture Radar: A Signal Processing Approach*, ISBN 0-7923-9677-4, Kluwer Academic Publishers, 1996.

[42] Fred M. Dickey, Armin W. Doerry, Louis A. Romero, "Degrading effects of the lower atmosphere on long range airborne SAR imaging," *IET Proceedings on Radar, Sonar & Navigation*, Vol. 1, No. 5, pp. 329–339, October 2007.

[43] M. R. Cook, S. D. Blunt, J.Jakabosky, "Optimization of waveform diversity and performance for pulse-agile radar," *Proceedings of the 2011 IEEE Radar Conference (RadarCon 2011)*, pp. 812-817, Kansas City, Missouri, USA, 23-27 May 2011.

[44] Armin W. Doerry, *Radar Receiver Oscillator Phase Noise*, Sandia National Laboratories Report SAND2018-3614, Unlimited Release, April 2018.

[45] James A. Scheer, James L. Kurtz, editors, *Coherent Radar Performance Estimation*, ISBN: 0-89006-628-0, Artech House, Inc., 1993.

[46] Armin W Doerry, *A Study of Pulse-Doppler Radar Pulse Repetition Frequency*, Sandia National Laboratories Report SAND2023-00771, Unlimited Release, March 2023.

[47] David Alan Garren, "Theory of Two-Dimensional Signature Morphology for Arbitrarily Moving Surface Targets in Squinted Spotlight Synthetic Aperture Radar," *IEEE Transactions on Geoscience And Remote Sensing*, Vol. 53, No. 9, pp. 4997-5008, September 2015.

[48] Justin B. Campbell, Francisco Pérez, Qi Wang, Balasubramaniam Santhanam, Ralf Dunkel, Armin W. Doerry, Thomas Atwood, Majeed M. Hayat, "Remote Vibration Estimation Using Displaced-Phase-Center Antenna SAR for Strong Clutter Environments," *IEEE Transactions on Geoscience and Remote Sensing*, Vol. 56, No. 5, pp. 2735-2747, May 2018.

[49] George T. Ruck, Donald E. Barrick, William D. Stuart, Clarence K. Krichbaum*, Radar Cross Section Handbook*, ISBN-13: 978-0306303432, Plenum Press, 1970.

[50] Pawan Setlur, Tadahiro Negishi, Natasha Devroye, Danilo Erricolo, "Multipath Exploitation in Non-LOS Urban Synthetic Aperture Radar," IEEE Journal of Selected Topics in Signal Processing, Vol. 8, No. 1, pp. 137-152, February 2014.

[51] Walter G. Carrara, Ron S. Goodman, Ronald M. Majewski, *Spotlight Synthetic Aperture Radar, Signal Processing Algorithms*, ISBN 0-89006-728-7, Artech House, Inc., 1995.

[52] Aimee Shore, John R. Summerfield, R. Derek West, Brandon Conder, Frederick W. Koehler, Wade Schwartzkopf, "Automated Impulse Response Detection and Analysis in Synthetic Aperture Radar Imagery," *Proceedings of the 2023 IEEE Radar Conference (RadarConf23)*, pp. 1-6, San Antonio, TX, USA, 1-5 May 2023.

[53] Donald R. Wehner, *High-Resolution Radar – Second Edition*, ISBN 0-89006-727-9, Artech House, Inc., 1995.

[54] Chris Oliver, Shaun Quegan, *Understanding Synthetic Aperture Radar Images*, ISBN: 0-89006-850-X, Artech House, Inc., 1998.

[55] Armin W Doerry, Douglas L Bickel, *Notes on Multilook for Filtering Speckle in Synthetic Aperture Radar Images*, Sandia National Laboratories Report SAND2022-12870, Unlimited Release, September 2022.

[56] Luis Gomez, Maria Elena Buemi, Julio C. Jacobo-Berlles, Marta E. Mejail, "A New Image Quality Index for Objectively Evaluating Despeckling Filtering in SAR Images," IEEE Journal of Selected Topics in Applied Earth Observations and Remote Sensing, Vol. 9, No. 3, PP. 1297-1307, March 2016.

[57] Armin W. Doerry, *Noise and Noise Figure for Radar Receivers*, Sandia National Laboratories Report SAND2016-9649, Unlimited Release, October 2016.

[58] A. W. Doerry, "Radiometric calibration of range-Doppler radar data," SPIE 2019 Defense & Commercial Sensing Symposium, *Radar Sensor Technology XXIII*, Vol. 11003, Baltimore, MD, 14-18 April 2019.

[59] Hans Hellsten, *Meter-Wave Synthetic Aperture Radar for Concealed Object Detection*, ISBN-13: 978-1-63081-025-2, Arthech House, 2017.

[60] International Telecommunications Union (ITU), *Radio Noise*, Recommendation ITU-R P.372-16, Geneva, August 2022.

[61] Maurice W. Long, *Radar Reflectivity of Land and Sea – Second Edition*, ISBN: 0-89006-130-0, Arthech House, Inc., 1983. (originally published by Lexington Books, 1975)

[62] Fawwaz T. Ulaby, M. Craig Dobson, *Handbook of Radar Scattering Statistics for Terrain*, ISBN: 0-89006-336-2, Artech House, Inc., 1989.

[63] Armin W. Doerry, *Performance Limits for Synthetic Aperture Radar – second edition*, Sandia National Laboratories Report SAND2006-0821, Unlimited Release, February 2006.

[64] Armin W. Doerry, *Collecting and Processing Data for High Quality CCD Images*, Sandia National Laboratories Report SAND2007-1545, Unlimited Release, March 2007.

[65] Armin W. Doerry, "Comments on radar interference sources and mitigation techniques," SPIE 2015 Defense & Security Symposium, Radar Sensor Technology XIX, Vol. 9461, Baltimore, MD, 20-24 April 2015.

[66] Fred E. Nathanson, *Radar Design Principles – second edition*, ISBN: 0-07-046052-3, McGraw-Hill, Inc., 1991.

[67] NGA Standardization Document, *Sensor Independent Complex Data (SICD) - Volume 1, Design & Implementation Description Document*, Version 1.1, National Center For Geospatial Intelligence Standards, 2014-09-30. (This is Volume 1 of a three volume set of documents.)

[68] Todd D. Penrod, Gilbert G. Kuperman, *Image Quality Analysis of Compressed Synthetic Aperture Radar Imagery*, United States Air Force Materiel Command Armstrong Laboratory Report AL/CF-TR-1993-0156, Unclassified, January 1993.

[69] Judi E. See, Gilbert G. Kuperman, *Effects of SAR Image Compression on Image Interpretability and Detection Performance*, United States Air Force Materiel Command Armstrong Laboratory Report AL/CF-TR-1996-0100, June 1996.

[70] D. L. Bickel, A. W. Doerry, "Using coherence as a quality measure for complex radar image compression," SPIE 2017 Defense & Security Symposium, *Radar Sensor Technology XXI*, Vol. 10188, Anaheim, CA, 9-13 April 2017.

[71] Armin W Doerry, *SAR Image Scaling, Dynamic Range, Radiometric Calibration, and Display*, Sandia National Laboratories Report SAND2019-2371, Unlimited Release, March 2019.

[72] G. L. LaMonica, *The Effects of Image Quality on Synthetic Aperture Radar Operator Performance – Volume 1 Target Recognition*, Air Force Avionics Laboratory Report AFAL-TR-74-333, Unclassified, March 1975.

[73] Leslie M. Novak, "Effects of Image Quality on SAR Target Recognition," *Radar Automatic Target Recognition (ATR) and Non-Cooperative Target Recognition (NCTR)*, edited by David Blacknell and Hugh Griffiths, ISBN: 978-1-84919-685-7, lectures from NATO STO-EN-SET-172-2013, The Institution of Engineering and Technology (IET), 2013.

[74] Roberto Casati, Patrick Cavanagh, Paulo E. Santos. "The Message in the Shadow: Noise or Knowledge? (Dagstuhl Seminar 15192)." *Dagstuhl Reports*, Vol. 5, No. 5., Schloss Dagstuhl-Leibniz-Zentrum fuer Informatik, 2015.

[75] A. M. Raynal, D. L. Bickel, A. W. Doerry, "Stationary and moving target shadow characteristics in synthetic aperture radar," Proceedings of the SPIE 2014 Defense & Security Symposium, *Radar Sensor Technology XVIII*, Vol. 9077, Baltimore MD, 5–9 May 2014.

[76] John Miller, Edward Bishop, Armin W. Doerry, Ann M. Raynal, "Impact of Ground Mover Motion and Windowing on Stationary and Moving Shadows in Synthetic Aperture Radar Imagery," Proceedings of the SPIE 2015 Defense & Security Symposium, *Algorithms for Synthetic Aperture Radar Imagery XXII*, Vol. 9475, Baltimore, MD, 20-24 April 2015.

[77] John M. Irvine, "National Imagery Interpretability Rating Scales (NIIRS): Overview and Methodology," Proceedings of the SPIE Optical Science, Engineering and Instrumentation '97, *Airborne Reconnaissance XXI*, Vol. 3128, pp. 93-103, San Diego, CA, USA, 27 July - 1 August 1997.

[78] Jerry D. Greer, Jule Caylor, "Development of an environmental image interpretabifity rating scale," Proceedings of the SPIE San Diego '92, *Airborne Reconnaissance XVI*, Vol. 1763, pp. 151-157, San Diego, CA, USA, 22 July 1992.

[79] Gilbert G. Kuperman, Dorit Shaya, *Subjective Assessment of SAR Imagery Enhancement Algorithms*, United States Air Force Armstrong Laboratory Report AL/CF-TR-1997-0133, September 1997.

[80] National Geospatial-Intelligence Agency, *National Imagery Interpretability Rating Scale Standard – Version 1.1.2*, National System for Geospatial Intelligence Standardization Document, NGA.STND. 0040_1.1.2, 4 December 2019.

[81] Ronald G. Driggers, James A. Ratches, Jon C. Leachtenauer, Regina W. Kistner, "Synthetic aperture radar target acquisition model based on a National Imagery Interpretability Rating Scale to probability of discrimination conversion," *Optical Engineering*, Vol. 42, No. 7, pp. 2104-2112, July 2003.

[82] Daniel Gutchess, John M. Irvine, Mon Young, Magnús S. Snorrasona, "Predicting the Effectiveness of SAR Imagery for Target Detection," Proceedings of the SPIE Defense, Security, and Sensing Symposium, *Algorithms for Synthetic Aperture Radar Imagery XVIII*, Vol. 8051, Orlando, Florida, USA, 25-29 April 2011.

[83] Wade Schwartzkopf, Jason Brown, Gordon Farquharson, Craig Stringham, Michael Duersch, Jordan Heemskerk, "Radar Generalized Image Quality Equation Applied to Capella Open Dataset," *Proceedings of the 2022 IEEE Radar Conference (RadarConf22)*, 21 March 2022.

[84] Arnold Jan den Dekker and A. van den Bos, "Resolution: a survey," *J. Opt. Soc. Am. A*, Vol. 14, No. 3, pp. 547-557, March 1997.

[85] Lord Rayleigh, "Investigations in optics, with special reference to the spectroscope,'' *Philosophical Magazine and Journal of Science*, Vol. 8, No. 49, pp. 261-274, October 1879.

[86] William V. Houston, "A Compound Interferometer for Fine Structure Work," *Physical Review*, Vol. 29, No. 3, pp. 478-485, March 1927.

[87] John C. Curlander, Robert N. McDonough, *Synthetic Aperture Radar: Systems and Signal Processing*, ISBN-13: 978-0471857709, John Wiley & Sons, Inc., 1991.

[88] Carroll Mason Sparrow, "On Spectroscopic Resolving Power," *The Astrophysical Journal*, Vol. 44, pp. 76-87, September 1916.

[89] Jack Capon, "High-resolution frequency-wavenumber spectrum analysis," *Proceedings of the IEEE*, Vol. 57, No. 8, pp.1408-1418, August 1969.

[90] Harry L. Van Trees, *Optimum Array Processing: Part IV of Detection, Estimation, and Modulation Theory*, ISBN-13: 978-0471093909, John Wiley & Sons, Inc., 2002.

[91] Christ D. Richmond, "Capon algorithm mean-squared error threshold SNR prediction and probability of resolution," *IEEE Transactions on Signal Processing*, Vol. 53, No. 8, pp.2748-2764, August 2005.

[92] Lars M. H. Ulander, Hans Hellsten, "A New Formula for SAR Spatial Resolution," *AEÜ - International Journal of Electronics and Communications*, Vol. 50, No. 2, pp. 117-121, March 1996.

[93] Armin W Doerry, *Bistatic Synthetic Aperture Radar – Issues, Analysis, and Design*, Sandia National Laboratories Report SAND2020-9992, Unlimited Release, September 2020.

[94] Viet T. Vu, "Area Resolution for Bistatic Ultrawideband Ultrawidebeam SAR," *IEEE Transactions on Aerospace and Electronic Systems*, Vol. 57, No. 2, pp.1371-1377, April 2021.

Distribution

Unlimited Release

Email—Internal

all members	0534x	
Technical Library	01911	sanddocs@sandia.gov

Sandia National Laboratories is a multimission laboratory managed and operated by National Technology & Engineering Solutions of Sandia LLC, a wholly owned subsidiary of Honeywell International Inc. for the U.S. Department of Energy's National Nuclear Security Administration under contract DE-NA0003525.